Ternary Phenolate-Based Thiosemicarbazone Complexes of Copper(II): Magnetostructural Properties, Spectroscopic Features and Marked Selective Antiproliferative Activity Against Cancer Cells

Iman K. Al-Salmi and Musa S. Shongwe *

Posted Date: 20 December 2023

doi: 10.20944/preprints202312.1515.v1

Keywords: mononuclear and dinuclear ternary copper(II) complexes; thiosemicarbazone; X-ray structures; tetragonal distortion; intermolecular forces; spectroscopy; selective potent cytotoxicity

Article

Ternary Phenolate-Based Thiosemicarbazone Complexes of Copper(II): Magnetostructural Properties, Spectroscopic Features and Marked Selective Antiproliferative Activity against Cancer Cells

Iman K. Al-Salmi and Musa S. Shongwe *

Department of Chemistry, College of Science, Sultan Qaboos University, PO Box 36, Al-Khod 123, Muscat, Sultanate of Oman

* Correspondence: musa@squ.edu.om; Tel.: +968-24142376

Abstract: The new diprotic ligand 3,5-di-*tert*-butylsalicylaldehyde 4-ethyl-3-thiosemicarbazone, abbreviated H_2(3,5-*t*-Bu_2)-sal4eT, exists as the thio-keto tautomer and adopts the *E*-configuration with respect to the imine double bond as evidenced by single-crystal X-ray analysis and corroborated by spectroscopic characterisation. Upon treatment with $Cu(OAc)_2{\cdot}H_2O$ in the presence of either 2,9-dimethyl-1,10-phenanthroline (2,9-Me_2-phen) or 1,10-phenanthroline (phen) as a co-ligand in MeOH, this thiosemicarbazone undergoes conformational transformation (relative donor-atom orientations: *syn,anti* → *syn,syn*) concomitantly with tautomerization and double deprotonation to afford the ternary copper(II) complexes [Cu{(3,5-*t*-Bu_2)-sal4eT}(2,9-Me_2-phen)] (**1**) and [Cu_2{3,5-*t*-Bu_2)-sal4eT}$_2$(phen)] (**2**). Crystallographic elucidation has revealed that complex **1** is a centrosymmetric dimer of mononuclear copper(II) complex molecules brought about by intermolecular H-bonding. The coordination geometry at the copper(II) centre is best described as distorted square pyramidal in accord with the trigonality index (τ = 0.14). The co-ligand adopts an axial-equatorial coordination mode; hence there is a disparity between its two Cu–N coordinate bonds arising from weakening of the apical one as a consequence of the tetragonal distortion. The axial X-band ESR spectrum of complex **1** is consistent with retention of this structure in solution. Complex **2** is a centrosymmetric dimer of dinuclear copper(II) complex molecules exhibiting intermolecular H-bonding and π-π-stacking interactions. The two copper(II) centres, which are 4.8067(18) Å apart and bridged by the thio-enolate nitrogen of the quadridentate thiosemicarbazonate ligand, display two different coordination geometries, one distorted square planar (τ_4 = 0.082) and the other distorted square pyramidal (τ_5 = 0.33). Such dinuclear copper(II) thiosemicarbazone complexes, which are crystallographically characterised, are extremely rare. *In vitro*, complexes **1** and **2** outperform cisplatin as antiproliferative agents in terms of potency and selectivity towards HeLa and MCF-7 cancer cell lines.

Keywords: mononuclear and dinuclear ternary copper(II) complexes; thiosemicarbazone; X-ray structures; tetragonal distortion; intermolecular forces; spectroscopy; selective potent cytotoxicity

1. Introduction

Thiosemicarbazones are multi-purpose hydrazone ligands of considerable interest in coordination chemistry [1]. Their characteristic functionality feature $R^1R^2C{=}N{-}N(H){-}C(=S){-}NR^3R^4$ is derived from the straightforward single-step Schiff-base condensation reaction between an aldehyde or a ketone and a thiosemicarbazide. Amongst their fascinating structural attributes is their coordination versatility arising from their propensity to undergo concomitant base-/metal-assisted tautomeric transformation and deprotonation as a means to meet charge-neutrality requirements. Moreover, a given thiosemicarbazone is capable of exhibiting different denticities and coordination modes as demanded by the metal centre [2–9]. By strategically employing aldehydes or ketones with

 doi:10.20944/preprints202312.1515.v1

moieties bearing donor atoms of interest in appropriate coordination positions, they can be tailor-designed for specially desired hetero-donor environments, coordination spheres [10], physicochemical features and biological properties [3,8,9,11–27]. Substituent groups can impart electronic effects to thiosemicarbazone complexes with interesting impact on physicochemical and pharmacological properties. The literature is replete with examples of thiosemicarbazone complexes exhibiting a broad spectrum of pharmacological properties including antitumour [3,8,9,11–22], antibacterial [20,21,23], antiviral [24,25], antifungal [23,26] and antimalarial [22,27].

Thiosemicarbazones stabilize predominantly metal ions from the *p*-, *d*- and *f*-blocks [1]; some of the transition-metal thiosemicarbazone complexes exhibit fascinating magneto-structural [28] and catalytic [29] properties amongst other features. Electrochemically, for copper (Z = 29; [Ar]4$s^1$3d^{10}), which is the subject of this paper, Schiff-base complexes shuttle between +1 and +2 oxidation states (Cu^{II}/Cu^{I} redox couple) [8,15,18,20,30]. Thiosemicarbazone complexes whose cyclic voltammograms exhibit these redox couples with potentials lying within the biologically accessible redox potential window ranging from –0.4 to +0.8 V *vs.* NHE [30], are of pharmacological importance in that they have the ability to generate intracellular reactive oxygen species (ROS) [8,15,18,20,30] desirable for apoptotic cytotoxicity. Ternary mononuclear complexes of copper(II) of the type [CuL(N,N-donor-L)]$^{n+}$ [where L represents a neutral or anionic polydentate primary ligand and N,N-donor-L stands for a heterocyclic bidentate N,N-donor chelating co-ligand such as 1,10-phenanthroline (phen), 2,2′-bipyridine (bipy), dipyridoquinoxaline (dpq), dipyridophenazine (dppz) or derivatives of these] abound [31–58]. Such coordination compounds are of considerable interest partly because of their potential to exhibit DNA binding/cleavage [34,39,41–44,50,51,53–55], anticancer [39,43,44,49,53,54] and antimicrobial [35–37,40] activities. Some have been explored as models for metallo-enzymes [33,45] while others have been designed to investigate structural and spectroscopic features of interest [4,32,38,46–48,52,56–58]. There is a paucity of crystallographically characterised ternary copper(II) thiosemicarbazone complexes of this type [4,31–39].

In this work, we have synthesized and structurally characterised the ligand 3,5-di-*tert*-butylsalicylaldehyde 4-ethyl-3-thiosemicarbazone, H_2(3,5-*t*-Bu_2)-sal4eT. Reaction of copper(II) ion with this ligand and the co-ligand 2,9-dimethyl-1,10-phenanthroline (2,9-Me_2-phen) or 1,10-phenanthroline (phen) in equimolar amounts produced the ternary copper(II) complex [Cu{(3,5-*t*-Bu_2)-sal4eT}(2,9-Me_2-phen)] (**1**) or [Cu_2{3,5-*t*-Bu_2)-sal4eT}$_2$(phen)] (**2**), respectively. The 3-D structures have been determined by single-crystal X-ray analyses. Whereas complex **1** is mononuclear, complex **2** is dinuclear. In the crystal lattice each exists as a dimer arising from two symmetrically-related intermolecular H-bonding interactions. To the best of our knowledge, [Cu_2{3,5-*t*-Bu_2)-sal4eT}$_2$(phen)] (**2**) is one of only two examples of crystallographically characterised dinuclear copper(II) thiosemicarbazone complexes of this kind. The other is [Cu_2(sal4eT)$_2$(bipy)], previously designated [$Cu_2(L^2)_2$(bipy) (bipy = 2,2′-bipyridine) [4]. While complex **2** is a centrosymmetric dimer of dinuclear complexes, the crystallographic asymmetric unit of [Cu_2(sal4eT)$_2$(bipy)] consists of two independent intramolecularly hydrogen-bonded dinuclear complex molecules. In both **2** and [Cu_2(sal4eT)$_2$(bipy)], the two copper(II) ions are in different coordination spheres. These two complexes differ in the five-coordinate geometry. The antiproliferative activity of complexes **1** and **2** along with H_2(3,5-*t*-Bu_2)-sal4eT has been tested against the cancer cell lines MCF-7 (human breast adenocarcinoma) and HeLa (human cervical carcinoma). Whereas the ligand is inactive against HeLa and MCF-7 cancer cells, the complexes are highly potent and selective.

2. Results and Discussion

2.1. Synthesis and Chemical Identification of the Thiosemicarbazone Ligand

The thiosemicarbazone H_2(3,5-*t*-Bu_2)-sal4eT was synthesised from equimolar amounts of 3,5-di-*tert*-butylsalicylaldehyde and 4-ethyl-3-thiosemicarbazide by the usual single-step Schiff-base condensation reaction in refluxing absolute ethanol. The resultant light yellow solution afforded long lustrous colourless needles upon slow evaporation of the solvent under ambient conditions over a span of several days. Unlike the synthesis of pyridyl-based thiosemicarbazones [8,13–15], this

Preprints (www.preprints.org) | NOT PEER-REVIEWED | Posted: 20 December 2023 doi:10.20944/preprints202312.1515.v1

phenolic thiosemicarbazone was produced straightforwardly in high yield without requiring acid-catalysis (Scheme 1). The chemical identity of this ligand was ascertained by microanalysis along with electrospray ionization (ESI) mass spectrometry. The ESI mass spectrum exhibits a parent peak at m/z = 334.3 $[M - H^+]^-$ in the negative-ion mode [Figure 1] and at m/z = 336.3 $[M + H^+]^+$ in the positive-ion mode, consistent with the molecular mass (M = 335.51 amu).

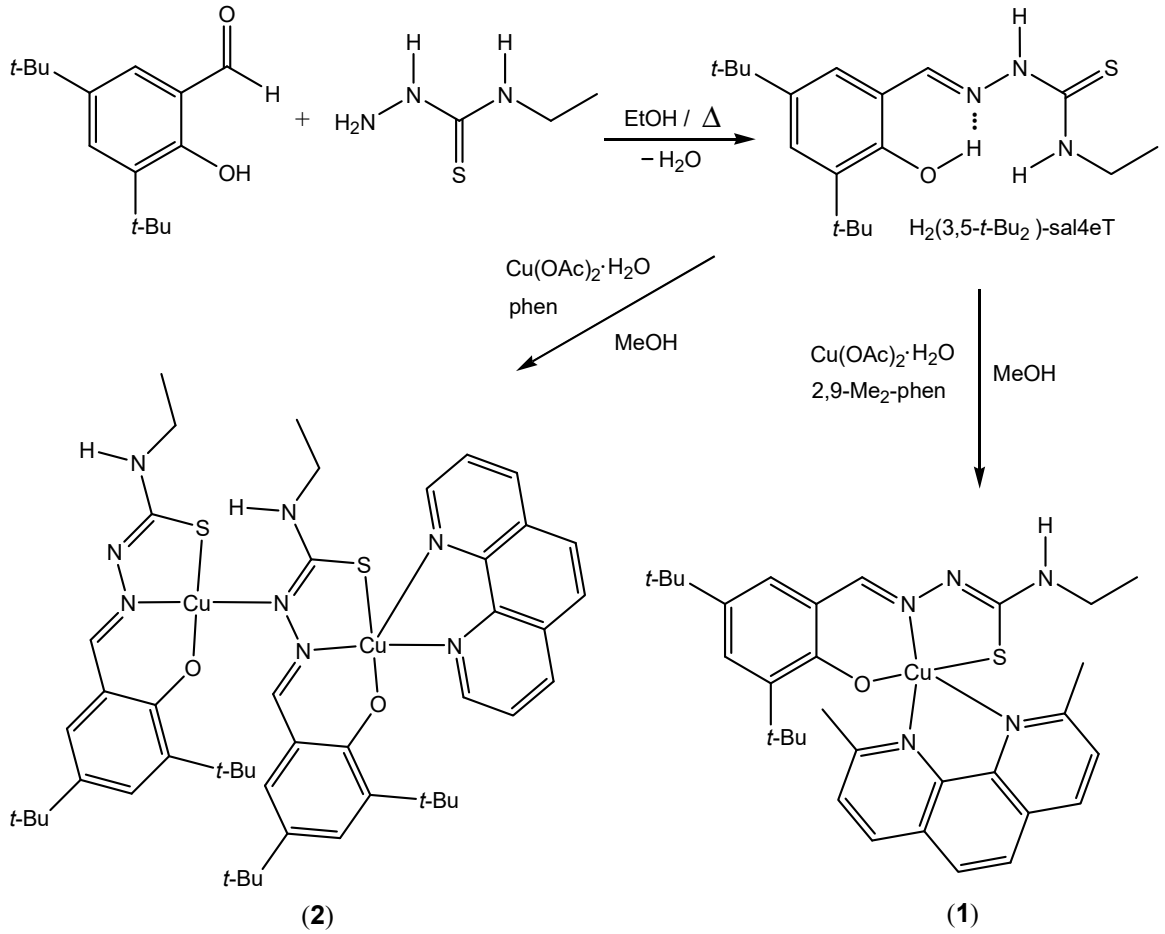

(**a**)

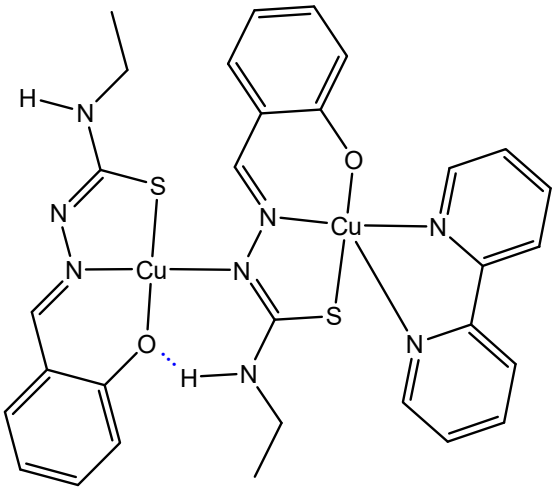

(**b**)

Scheme 1. (a) Illustration of synthetic routes to H_2(3,5-*t*-Bu_2)-sal4eT and complexes **1** and **2**; (b) comparative structural representation of [Cu_2(sal4eT)$_2$(bipy)] [4].

Preprints (www.preprints.org) | NOT PEER-REVIEWED | Posted: 20 December 2023 doi:10.20944/preprints202312.1515.v1

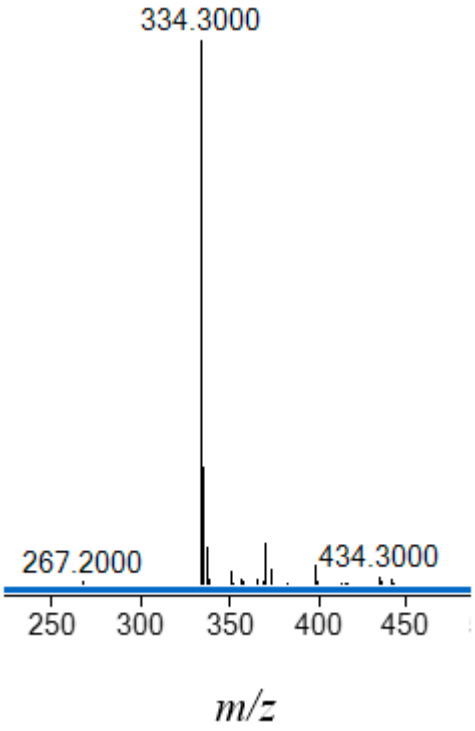

Figure 1. ESI mass spectrum of H_2(3,5-*t*-Bu_2)-sal4eT in the negative mode.

2.2. FT-IR and NMR Spectroscopic Characterization of the Thiosemicarbazone Ligand

That H_2(3,5-*t*-Bu_2)-sal4eT exists as the thio-keto (thione) tautomer in the solid state is demonstrated by the prominent IR absorption band at 3157 cm^{-1} indicative of the thio-amide ν(N–H) (Figure 2). The associated thio-carbonyl bond is characterised by the vibrational band with a stretching frequency of 1032 cm^{-1}. Indeed, the absence of a vibrational band around 2600 cm^{-1} due to ν(S–H) [10] excluded the possibility of the occurrence of the thio-enol tautomer. At 3320 cm^{-1} in the IR spectrum occurs an absorption band ascribable to the N–H stretch of the terminal secondary amino group of the thiosemicarbazone. A characteristic feature of Schiff bases is the imine bond whose presence in H_2(3,5-*t*-Bu_2)-sal4eT is evidenced by the absorption at 1609 cm^{-1} typifying ν(C=N). The *tert*-buyl C–H stretches are conspicuous by their characteristic pattern of absorption bands in the range 2867–2960 cm^{-1} [59]. Contributing to the intensity of these absorptions are the C–H vibrations of the *N*-ethyl substituent group. The sharp absorption band with the wavenumber 3013 cm^{-1} is attributable to the aromatic ν(C–H). Finally, the broad band around 3500 cm^{-1} is typical of phenolic C–O vibrations.

Preprints (www.preprints.org) | NOT PEER-REVIEWED | Posted: 20 December 2023 doi:10.20944/preprints202312.1515.v1

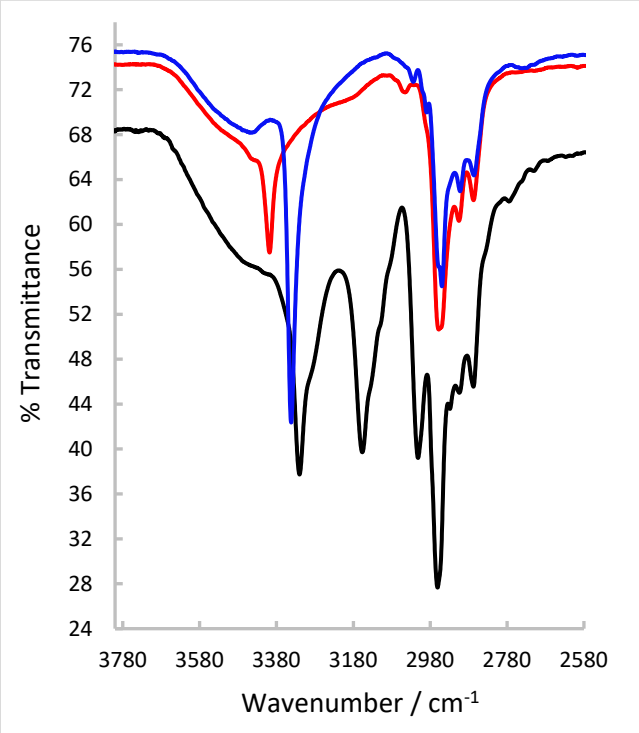

Figure 2. FT-IR spectra of (a) H_2(3,5-*t*-Bu_2)-sal4eT (black line) and (b) [Cu{3,5-*t*-Bu_2)-sal4eT}(2,9-Me_2-phen)] (**1**) (blue line) and [Cu_2{3,5-*t*-Bu_2)-sal4eT}$_2$(phen)] (**2**) (red line).

The ^{1}H-NMR spectrum of H_2(3,5-*t*-Bu_2)-sal4eT was recorded in DMSO-d_6 at a radiofrequency of 700 MHz with TMS as an internal reference standard (δ = 0). The broad peak at δ 9.98 assignable to the hydrazinic proton reveals that the thione tautomer of this thiosemicarbazone remains intact in solution. The phenolic proton, which is represented by the singlet at δ 11.27, is the most deshielded on account of its intramolecular interaction with the imine nitrogen atom. The aldimine proton is associated with the sharp singlet at δ 8.28. A broad resonance shaped like an unresolved triplet occurs at δ 8.48 and is attributable to the proton of the amino group between the thio-carbonyl and ethyl groups. The aromatic protons in positions 4 and 6 resonate as doublets at δ 7.13 and 7.29, respectively, with identical coupling constants (J = 2.38 Hz). The *N*-ethyl group is characterised by partially overlapping quartet signals at δ 3.59 (J = 6.55 Hz) and a triplet resonance at δ 1.16 (J = 7.14 Hz) corresponding to the methylene protons in non-equivalent environments and the methyl protons, respectively. Finally, the protons of the 3-*tert*-butyl and 5-*tert*-butyl substituent groups have singlet signals with the chemical shifts δ 1.41 and 1.27, respectively.

2.3. Single-Crystal X-ray Structure Determination of the Thiosemicarbazone Ligand

Definitive evidence for the solid-state 3-D structure of the ligand was provided by single-crystal X-ray analysis. A colourless needle amenable to X-ray diffraction was grown from a solution of H_2(3,5-*t*-Bu_2)-sal4eT in EtOH at room temperature. X-ray data collection was performed at 100 K. Crystal data, details of data collection and parameters for structure solution and refinement are compiled in Table 1. Evidently, this thiosemicarbazone ligand crystallized in the monoclinic space group $P2_1/c$ with four molecules in the unit cell. The X-ray crystal structure is depicted in Figure 3 while selected bond distances and angles are presented in Table 2. The distance of the Schiff-base bond C=N [C(15)–N(1) = 1.2904(19) Å] lies within the range observed for normal imine bonds [1.26–1.30 Å] [13–15,19,20,60–69] in non-coordinated ligands. Upon reduction of the Schiff base, the imine double bond becomes a single bond (C–N) with a distance of ~1.47 Å [65]. The C(16)–S(1) distance of 1.7029(14) Å verifies the occurrence of the thione tautomer. Literature values for the distance of the thio-carbonyl bond in free thiosemicarbazone ligands range typically from 1.65 to 1.70 Å [13–15,19,20,60–69] (even longer if involved in bifurcated H-bonding) [67]. Both imine nitrogen and thio-

 doi:10.20944/preprints202312.1515.v1

carbonyl carbon are sp^2-hybridised and the angles around them reflect the angular (with a lone pair) and trigonal planar geometries about these two atoms. The hydrazinic N–N bond [N(1)–N(2) = 1.3854(16) Å] is somewhat longer than most of those reported for other non-coordinated thiosemicarbazones and is consistent with single-bond character.

Table 1. Selected crystallographic data for H_2(3,5-*t*-Bu_2)-sal4eT and complexes **1** and **2**.

Compound	**H_2(3,5-*t*-Bu_2)-sal4eT**	**1**	**2**
Chemical formula	$C_{18}H_{29}N_3OS$	$C_{32}H_{39}CuN_5OS$	$C_{48}H_{62}Cu_2N_8O_2S_2$
Molar mass (g mol^{-1})	335.50	605.28	974.25
T (K)	100	99.99	100.01
Crystal system	monoclinic	monoclinic	triclinic
Space group	$P2_1/c$	$P2_1/n$	$P\bar{1}$
a (Å)	18.4754(14)	8.5924(3)	11.3898(6)
b (Å)	9.2040(7)	18.5809(6)	13.1195(8)
c (Å)	11.5714(9)	19.4132(6)	16.6701(10)
α (°)	90	90	78.980(2)
β (°)	95.517(2)	100.451(2)	89.824(2)
γ (°)	90	90	83.661(3)
V (Å^3)	1958.6(3)	3047.99(17)	2429.7(2)
Z	4	4	2
ρ_{calc} (g cm^{-3})	1.138	1.319	1.332
μ (mm^{-1})	0.173	1.904	2.241
F(000)	728.0	1276.0	1024.0
Crystal size (mm)	0.500 × 0.200 × 0.150	0.240 × 0.120 × 0.080	0.508 × 0.207 × 0.040
Radiation (λ/ Å)	MoKα (λ = 0.71073)	CuKα (λ = 1.54178)	CuKα (λ = 1.54178)
2Θ range (°)	4.43 – 57.282	6.638 – 133.168	5.402 – 133.766
Reflections collected	37828	19602	30501
R_{int}	0.0661	0.0918	0.0708
GOF on F^2	1.051	1.044	1.189
R_1, wR_2 [$I \geq 2\sigma$ (I)]	0.0403, 0.0909	0.0513, 0.1235	0.1083, 0.3568
R_1, wR_2 [all data]	0.0607, 0.1010	0.0749, 0.1378	0.1180, 0.3692

One of the prominent structural features of interest is the intramolecular H-bonding interaction between the phenolic –O–H group and the imine nitrogen atom [O(1)–H(1)···N(1): O1–H1 = 0.84 Å, H1···N1 = 1.98 Å, O1···N1 = 2.7221(15) Å, O1–H1···N1 = 147.4º]. Indeed, the vast majority of Schiff bases derived from 2-hydroxybenzaldehydes, 2-hydroxyacetophenones, 2-hydroxybenzophenones, 2-hydroxypropiophenones, etc. exhibit this intramolecular electrostatic force. It is well-established that pyridyl-/phenol-based thiosemicarbazones can adopt an *E*- or *Z*-configuration with respect to the imine double bond. Moreover, they can also orient themselves in different conformations as a consequence of free rotation about the C(py/phenol)–C(imine) [i.e. C(6)–C(15) in this structure] single bond and the amide N(H)–C(=S) [i.e. N(2)–((16) in this structure] single bond. Thus the potential donor atoms can be positioned *anti* or *syn* relative to each other. Examples of crystallographically observed orientations of phenolic thiosemicarbazones, *viz. E(syn,anti)* [60,62,63], *E(syn,syn)* [61,64]

Preprints (www.preprints.org) | NOT PEER-REVIEWED | Posted: 20 December 2023 doi:10.20944/preprints202312.1515.v1

and *E(ant,anti)* [63], are shown in Figure 3. The structure of H_2(3,5-*t*-Bu_2)-sal4eT is consistent with the *E*-configuration; the phenolic –OH group and the imine nitrogen are positioned *syn* to each other while the thione sulfur points to the opposite side in an *anti*-orientation relative to the imine nitrogen.

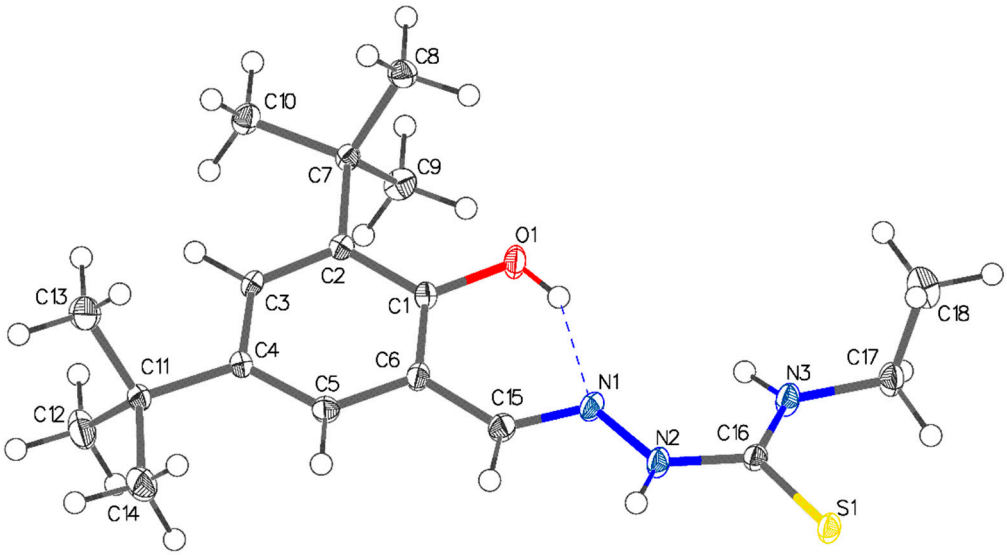

(**a**)

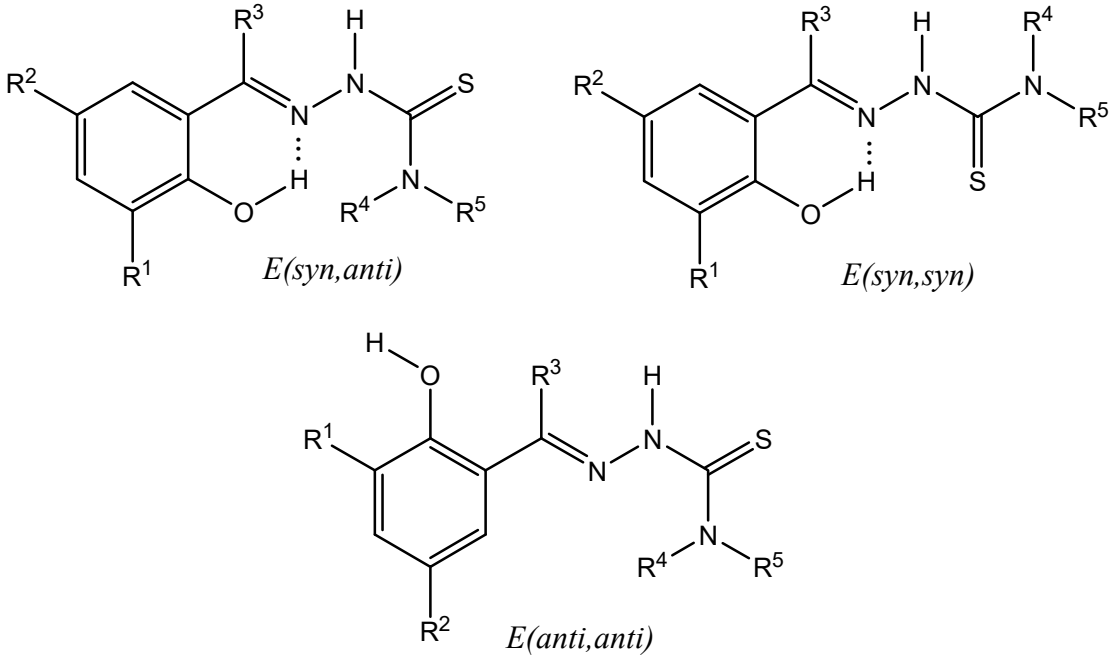

(**b**)

Figure 3. (a) X-ray crystal structure of H_2(3,5-*t*-Bu_2)-sal4eT and (b) illustrations of crystallographically observed different orientations of phenolic thiosemicarbazones.

Table 2. Selected bond distances (Å) and angles (°) for H_2(3,5-*t*-Bu_2)-sal4eT.

C16-S1	1.7029(14)
C1-O1	1.3605(16)

Preprints (www.preprints.org) | NOT PEER-REVIEWED | Posted: 20 December 2023 doi:10.20944/preprints202312.1515.v1

N1-N2	1.3854(16)
C15-N1	1.2904(19)
C16-N2	1.3499(18)
C15-N1-N2	113.66(12)
N2-C16-N3	118.40(13)
N2-C16-S1	117.87(11)
N3-C16-S1	123.72(11)

2.4. Synthesis and Chemical Identification of the Copper(II) Thiosemicarbazone Complexes

Reaction of H_2(3,5-*t*-Bu_2)-sal4eT with a molar equivalent of $Cu(OAc)_2{\cdot}H_2O$ in refluxing MeOH, followed immediately by addition of a stoichiometric amount of 2,9-dimethyl-1,10-phenanthroline (2,9-Me_2-phen) or 1,10-phenathroline (phen) with brief heating of the resultant dark olive green solution, afforded the mononuclear copper(II) complex [Cu{(3,5-*t*-Bu_2)-sal4eT}(2,9-Me_2-phen)] (**1**) or the dinuclear copper(II) complex [Cu_2{(3,5-*t*-Bu_2)-sal4eT}$_2$(phen)] (**2**), respectively. The chemical formulations of these two ternary complexes were established by elemental analyses. The positive-ion ESI mass spectrum of complex **1** presented in Figure 4(a) shows a molecular peak at *m*/*z* = 605.4 in agreement with the molecular mass of this complex (605.25 amu). As regards the dinuclear complex (**2**), the parent ion was not detected; however, the ESR spectrum revealed important structural information from the fragmentation pattern. In the negative mode, the spectrum shows a minor peak at *m*/*z* = 792.5 consistent with the loss of the phen co-ligand. At *m*/*z* = 730.5 occurs a major peak ascribable to the fragment $[Cu\{(3,5\text{-}Bu_2)\text{-}sal4eT\}_2]^{2-}$ indicative of a loss of $[Cu(phen)]^{2+}$ [Figure 4(b)]. On the other hand, the positive-ion ESI spectrum exhibits a peak at *m*/*z* = 732.6 attributable to the fragment $[Cu\{(3,5\text{-}t\text{-}Bu_2)\text{-}sal4eT\}_2]^{+}$. Further dissociation affords the fragment $[Cu\{(3,5\text{-}t\text{-}Bu_2)\text{-}sal4eT\}]^{+}$ observed at *m*/*z* = 397.2, signifying the loss of one of the thiosemicarbazonate ligands. That complexes **1** and **2** are molecular has been demonstrated by the negligible value of the molar electrical conductivity (Λ_M ~3 Ω^{-1} cm^2 mol^{-1}) of their nonelectrolyte solutions in MeOH, EtOH and DMF at room temperature [70].

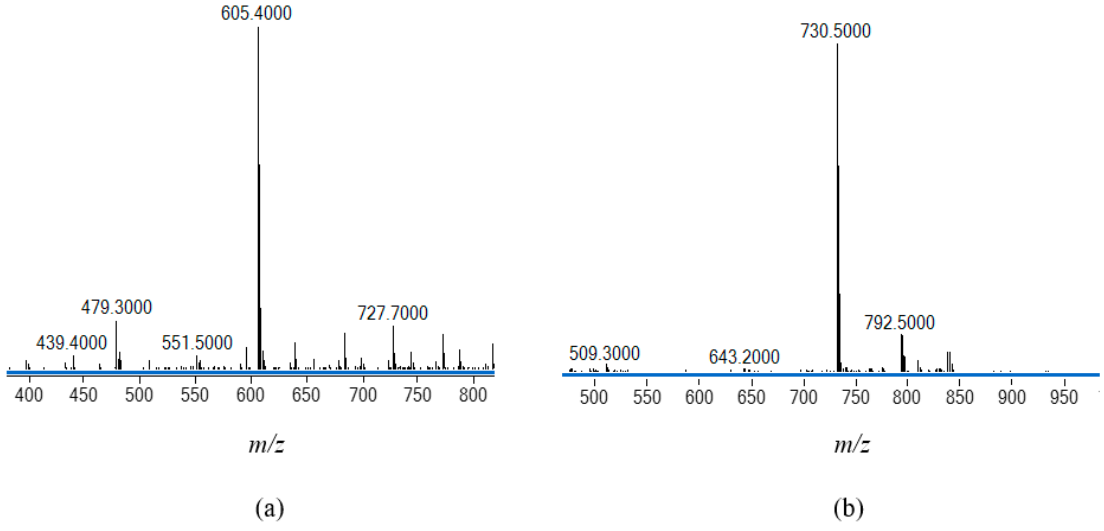

Figure 4. ESI mass spectra of (a) [Cu{(3,5-*t*-Bu_2)-sal4eT}(2,9-Me_2-phen)] (**1**) in the positive-ion mode and (b) [Cu_2{(3,5-*t*-Bu_2)-sal4eT}$_2$(phen)] (**2**) in the negative-ion mode.

2.5. FT-IR Spectroscopy and Magnetic Susceptibility Measurements

A comparison of the IR spectra of the thiosemicarbazone ligand and its copper(II) complexes (**1** and **2**) in Figure 3 shows clearly the absence of the vibrational band of the hydrazinic N–H bond from the spectra of the complexes. The disappearance of the hydrazinic proton coupled with the shift in

 doi:10.20944/preprints202312.1515.v1

the stretching frequency of the absorption band of the carbon-sulfur bond from 1032 cm^{-1} for the ligand to 842 and 858 cm^{-1} for **1** and **2**, respectively, is indicative of tautomerisation and deprotonation of the thiosemicarbazone upon coordination to the copper(II) ion, as is indeed necessary for charge-neutrality of the resultant complexes. The presence of the N–H group attached to the terminal ethyl group is proven by the occurrence of sharp absorption bands at 3398 and 3342 cm^{-1} in the spectra of **1** and **2**, respectively. The wavenumbers of the imine bond for **1** and **2** complexes are somewhat lower than that of the free ligand [ν(C=N): 1598 and 1599 cm^{-1} *vs.* 1609 cm^{-1})] consistent with coordination of the imine donor atom. Interestingly, the ν(N–N) absorptions for the ligand and complexes **1** and **2** virtually coincide (1172, 1170 and 1169 cm^{-1}, respectively), implying minimal delocalisation of π-electrons, if any, along the ligand backbone in the complexes. Finally, the other ligand IR absorption patterns, especially those of the *tert*-butyl C–H bonds (2850–2960 cm^{-1}), are retained.

Complexes **1** and **2** are paramagnetic with a single unpaired electron at the metal centre in the ground state. The room-temperature effective magnetic moment [$\mu_{eff} = (8\chi_M)^{½}$] of the mononuclear complex (**1**) is 1.83 μ_B. It is comparable with the spin-only value [$\mu_S = \{4S(S + 1)\}^{½}$, where $S = ½$] and lies within the range of literature values [45,50,54,56–59]. In contrast, for the dinuclear complex (**2**), μ_{eff} = 2.38 μ_B at room temperature, which is close to the spin-only value for two magnetically uncoupled d^9 paramagnetic centres [$\{4S_1(S_1 + 1) + 4S_2(S_2 + 1)\}^{½}$, where $S_1 = S_2 = ½$].

2.6. Single-Crystal X-ray Analyses of the Ternary Copper(II) Complexes

For each of the complexes [Cu{(3,5-*t*-Bu_2)-sal4eT}(2,9-Me_2-phen)] (**1**) and [Cu_2{(3,5-*t*-Bu_2)-sal4eT}$_2$(phen)] (**2**), X-ray diffraction data were collected on a single crystal at 100 K employing Cu-Kα radiation (λ = 1.54178 Å). Crystal data together with details of data collection and structure refinement are presented in Table 1. Selected bond distances and angles are given in Table 3. Whereas complex **1** crystallised in the monoclinic space group $P2_1/n$ with $Z = 4$, complex **2** did so in the triclinic space group $P\bar{1}$ with two complex molecules in the unit cell. Both complexes **1** and **2** do not possess solvent molecules of crystallisation.

The crystal structure of [Cu{(3,5-*t*-Bu_2)-sal4eT}(2,9-Me_2-phen)], depicted in Figure 5, reveals that this complex exists as a centrosymmetric dimer of mononuclear molecular ternary complexes of copper(II). The dimerisation occurs by two intermolecular hydrogen-bonding interactions involving the –N^4–H group of one complex molecule and the thio-enolate sulfur of the other complex molecule [Figure 5(b)] [N(3)–H(3)···S(1): N–H = 0.88 Å, H···S = 2.64 Å, N···S = 3.482(3) Å, N–H–S = 159.9º (symmetry code: 1–*x*, 1–*y*, –*z*)]. The charge-neutrality of this ternary complex implies that the thiosemicarbazone been doubly deprotonated upon complexation. Indeed transformation of the ligand from the thio-keto tautomer to the thio-enolate anion is demonstrated by the changes to the lengths of the pertinent bonds of the thio-amide. The thio-amide N–C bond [N(2)–C(16): 1.3499(18) Å] in the free ligand has shortened considerably upon complexation [N(2)–C(8): 1.313(4) Å in complex **1**] while the thio-carbonyl (C=S) bond [C(16)–S(1): 1.7029(14) Å] has converted to thio-enolate C–S^- bond in the complex [C(8)–S(1) = 1.739(3) Å]. Carbon-nitrogen bonds with double-bond character have been reported to have distances in the range 1.27–1.32 Å [66,71–73] when the N donor atom is coordinated to a central metal ion. On the other hand, typical lengths of carbon-sulfur bonds with single-bond character in thio-enolate complexes are in the range 1.72–1.77 Å [66,71–73]. The distances of the imine C=N [C(7)–N(1) = 1.296(4) Å] and the hydrazinic N–N [N(1)–N(2) = 1.400(4) Å] in **1** are normal with respect to their respective bond orders.

Table 3. Selected bond distances (Å) and angles (°) for **1** and **2**.

[Cu{(3,5-*t*-Bu_2)-sal4eT}(2,9-Me_2-1,10-phen)] (1)			
Cu(1)-S(1)	2.2823(9)	S(1)-C(8)	1.739(3)
Cu(1)-O(1)	1.934(2)	N(2)-C(8)	1.313(4)
Cu(1)-N(1)	1.959(3)	N(1)-N(2)	1.400(4)
Cu(1)-N(4)	2.057(3)	N(1)-C(7)	1.296(4)

Preprints (www.preprints.org) | NOT PEER-REVIEWED | Posted: 20 December 2023 doi:10.20944/preprints202312.1515.v1

Cu(1)-N(5)	2.308(3)	N(3)-C(8)	1.357(4)
O(1)-Cu(1)-N(1)	91.55(10)	N(1)-Cu(1)-N(4)	172.64(11)
N(1)-Cu(1)-S(1)	84.77(8)	N(1)-Cu(1)-N(5)	109.81(11)
O(1)-Cu(1)-N(4)	90.08(10)	N(4)-Cu(1)-S(1)	91.76(7)
O(1)-Cu(1)-N(5)	98.14(10)	N(5)-Cu(1)-S(1)	97.38(7)
O(1)-Cu(1)-S(1)	164.38(8)	N(4)-Cu(1)-N(5)	77.04(11)
[Cu_2{(3,5-*t*-Bu_2)-sal4eT}$_2$(phen)] (2)			
Cu(1)-S(1)	2.266(3)	Cu(2)-S(2)	2.231(3)
Cu(1)-O(1)	1.908(7)	Cu(2)-O(2)	1.888(7)
Cu(1)-N(1)	1.952(8)	Cu(2)-N(2)	2.017(8)
Cu(1)-N(4)	2.039(8)	Cu(2)-N(6)	1.940(8)
Cu(1)-N(5)	2.276(9)	N(6)-C(37)	1.310(12)
S(1)-C(8)	1.737(9)	S(2)-C(38)	1.746(9)
N(2)-C(8)	1.322(13)	N(7)-C(38)	1.316(12)
N(1)-C(7)	1.301(13)	N(6)-N(7)	1.391(11)
N(1)-N(2)	1.381(11)	N(8)-C(38)	1.353(13)
O(1)-Cu(1)-N(1)	93.7(3)	N(5)-Cu(1)-S(1)	102.9(2)
N(1)-Cu(1)-S(1)	85.2(2)	N(4)-Cu(1)-N(5)	77.7(3)
O(1)-Cu(1)-N(4)	89.7(3)	O(2)-Cu(2)-N(2)	88.1(3)
O(1)-Cu(1)-N(5)	104.6(3)	O(2)-Cu(2)-N(6)	94.2(3)
O(1)-Cu(1)-S(1)	152.4(2)	N(2)-Cu(2)-N(6)	176.3(3)
N(1)-Cu(1)-N(4)	172.2(4)	S(2)-Cu(2)-N(2)	91.8(2)
N(1)-Cu(1)-N(5)	94.6(3)	S(2)-Cu(2)-N(6)	86.3(2)
N(4)-Cu(1)-S(1)	95.1(2)	S(2)-Cu(2)-O(2)	172.1(3)

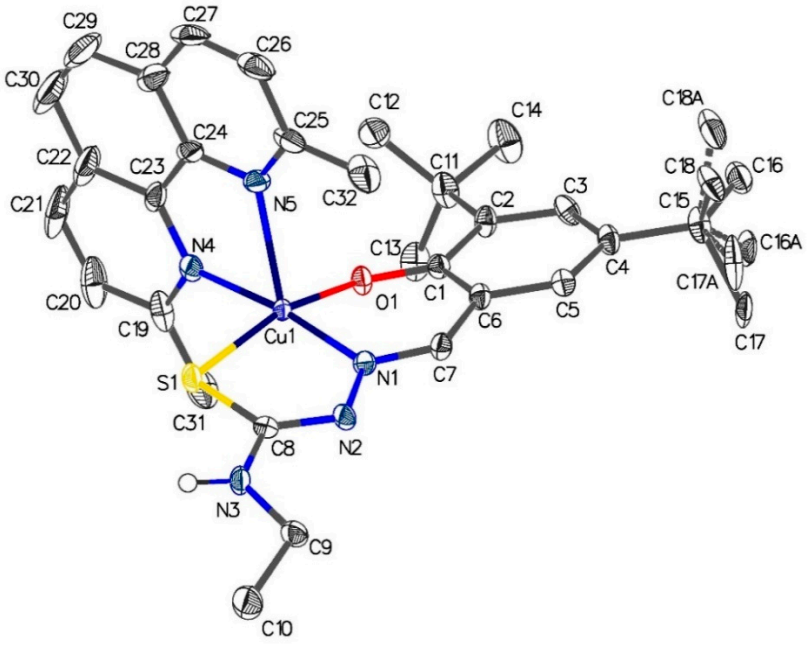

(a)

Preprints (www.preprints.org) | NOT PEER-REVIEWED | Posted: 20 December 2023 doi:10.20944/preprints202312.1515.v1

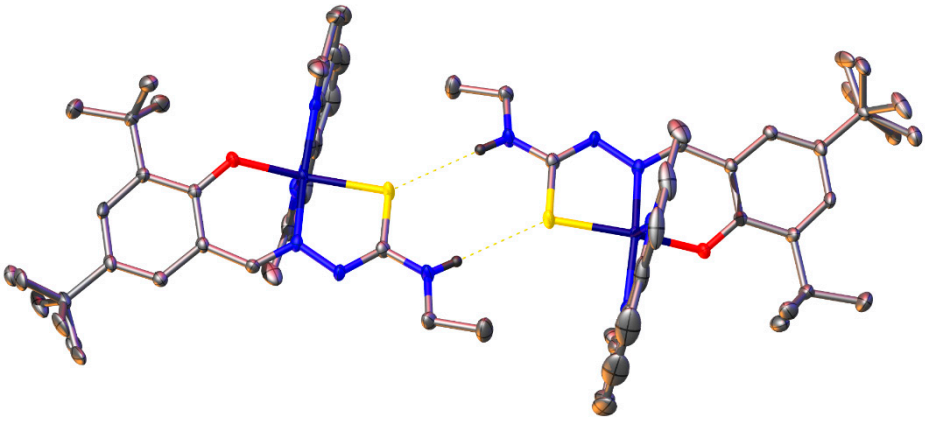

(b)

Figure 5. (a) Molecular structure of [Cu{(3,5-*t*-Bu$_2$)-sal4eT}(2,9-Me$_2$-phen)] (**1**) and (b) illustration of dimerization of the mononuclear complex molecules.

The five-coordinate geometry at the copper(II) centre arises from the tridentate coordination of the thiosemicarbazonate ligand with the donor atoms, namely phenolate oxygen, imine nitrogen and thio-enolate sulfur, arranged meridionally and the bidentate coordination of the 2,9-Me$_2$-phen co-ligand oriented nearly perpendicularly relative to the primary ligand. The axial-equatorial coordination mode of pyridyl nitrogen atoms of 2,9-Me$_2$-phen leads to the construction of a coordination sphere best described as distorted square pyramidal in accord with the trigonality index [$\tau = (\beta - \alpha)/60^{o}$] [74] of ~0.14, the largest two angles β and α being in the basal plane. The axial Cu–N bond is considerably longer than the one lying equatorially [Cu–N$_{ax\ (co\text{-}ligand)}$ = 2.308(3) Å *vs*. Cu–N$_{eq\ (co\text{-}ligand)}$ = 2.057(3) Å]. This elongation of the axial coordinate bond is attributable to the tetragonal distortion at the metal centre. Invariably, square pyramidal [31–43,45–52] and octahedral [44,53] ternary complexes with axial-equatorial coordination of bidentate co-ligand (bipy, phen or their derivatives) are subject to the Jahn-Teller effect evidenced by this structural feature. In some cases, even binary bis(chelate) copper(II) complexes [75] with two potentially tridentate ligands experience this effect, causing one of the ligands to coordinate bidentately due to considerable weakening of one of the axial Cu–L bonds. The magnitude of the disparity in the Cu–N distances of the asymmetrically coordinated N,N-donor co-ligand is in the range ~0.22–0.32 Å. Moreover, the complex cation of tris(1,10-phenanthroline)copper(II) perchlorate [76] exhibits Jahn-Teller distortion (Cu–N bond averages: Cu–N$_{ax}$ ~2.33 Å *vs*. Cu–N$_{eq}$ ~2.04 Å) whereby the axial Cu–N$_{phen}$ bonds are elongated to the same extent as those in the above-mentioned square pyramidal copper(II) ternary complexes. In contrast, it has been crystallographically proven that the two Cu–N bonds of N,N-donor co-ligands in square pyramidal and octahedral complexes where they lie on the equatorial plane are virtually equivalent as neither is subject to the Jahn-Teller effect [54–58]. In addition, in the complex [Cu{N(CN)$_2$}(phen)$_2$]$^+$ [77] with a distorted *trigonal bipyramidal* geometry at the metal centre the phen Cu–N distances are virtually indistinguishable from each other as the Jahn-Teller effect does not apply. The copper(II) ion in [Cu{(3,5-*t*-Bu$_2$)-sal4eT}(2,9-Me$_2$-phen)] (**1**) is displaced out of the mean basal plane [(N(1), S(1), O(1), N(4)] towards the apical phen N(5) donor atom by 0.1998(12) Å. Finally, the magnetostructural behaviour of this complex is consistent with half occupancy of the d_{x2-y2} orbital in the ground state.

As can be seen from Figure 6, [Cu$_2${(3,5-*t*-Bu$_2$)-sal4eT}$_2$(phen)] (**2**) exists in the crystal lattice as a centrosymmetric dimer of dinuclear molecular ternary complexes of copper(II) stabilized mainly by two types of intermolecular forces. The linkage of two dinuclear complex molecules occurs through two H-bonds between the N^4–H group of one dinuclear molecule and the imine nitrogen of another dinuclear molecule [N(3)–H(3)···N(7): N–H = 0.88 Å, H···N = 2.17 Å, N···N = 2.964(11) Å, N–H···N = 150.5º (symmetry code: 2–*x*, –*y*, 1–*z*)]. Moreover, this complex exhibits π-π stacking interactions

Preprints (www.preprints.org) | NOT PEER-REVIEWED | Posted: 20 December 2023 doi:10.20944/preprints202312.1515.v1

involving the plane N(5), C(24)–C(28) of the phen co-ligand in two complex molecules (symmetry code: 1–*x*, 1–*y*, 1–*z*) [angle of interaction of the two planes = 0.0(7)º, centroid-to-centroid distance = 6.603(8) Å, shift distance = 1.218(17) Å] (Figure S1).

The two copper(II) centres are 4.8067(18) Å apart and display different coordination numbers, one four-coordinate and the other five-coordinate, the respective coordination geometries being distorted square planar [$\tau_4 = \{360º - (\alpha + \beta)\}/141º = 0.082$, $\alpha = 176.3º$ and $\beta = 172.1º$] [78] and distorted square pyramidal [$\tau_5 = (\beta - \alpha)/60º = 0.33$, $\beta = 172.4º$ and $\alpha = 152.4º$] [74]. The two associated thiosemicarbazonate ligands exhibit different denticities: one coordinates in a tridentate fashion to the metal centre, [Cu(2) in Figure 6] with coordination number 4 whereas the other adopts the relatively unusual quadridentate coordination mode to bridge the two metal centres with the thio-enolate nitrogen atom, N(2), and coordinate meridionally to the other metal centre [Cu(1) in Figure 6]. For the tridentate ligand, coordinated to Cu(2), the distance of the newly-formed thio-enolate N=C bond is virtually indistinguishable from that of the imine C=N bond (*cf.* N(7)–C(38) = 1.316(12) Å *vs.* C(37)–N(6) = 1.310(12) Å, respectively] and the distance of C(32)–S(2) [1.746(9) Å] lies within the range reported for such thio-enolate bonds. Similarly, for the quadridentate ligand, the distances of the thio-enolate N=C and imine C=N bonds compare favourably [*cf.* N(2)–C(8) = 1.322(13) Å and C(7)–N(1) = 1.301(13) Å, respectively] [66,71–73]. The distance of the thio-enolate C–S$^-$ bond [C(8)–S(1) = 1.737(9) Å is normal for complexed thiosemicarbazonate ligands [66,71–73]. It is noteworthy that the lengths of the hydrazinic N–N bonds in this dinuclear complex [N(1)–N(2) = 1.381(11) Å and N(6)–N(7) = 1.391(11) Å] are very similar to that observed in the free ligand as a thio-keto (thione) tautomer [1.3854(16) Å], suggesting that there is no delocalization of electrons involving this chemical bond in the thiosemicarbazonate backbone.

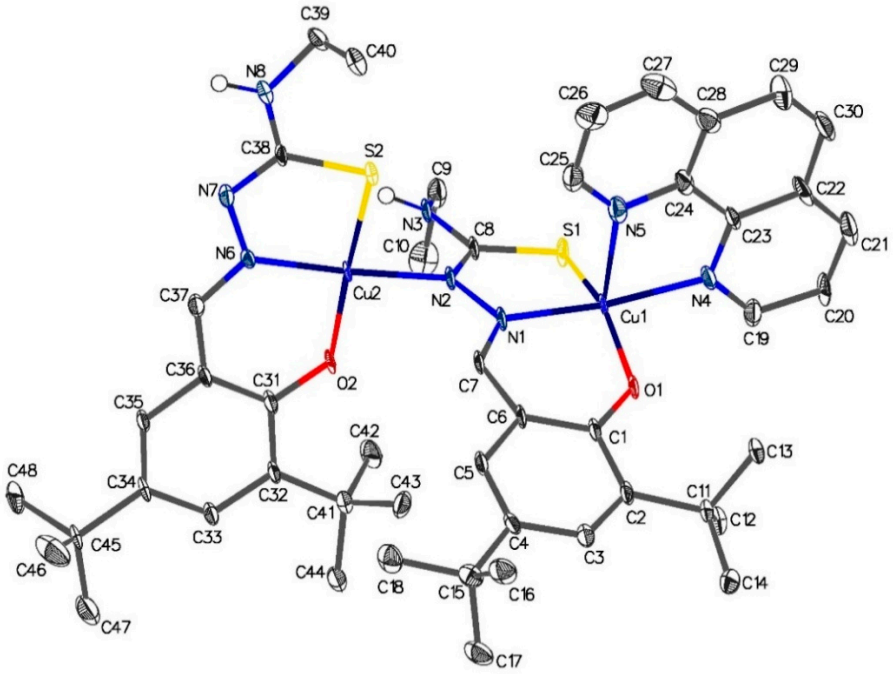

(a)

Preprints (www.preprints.org) | NOT PEER-REVIEWED | Posted: 20 December 2023 doi:10.20944/preprints202312.1515.v1

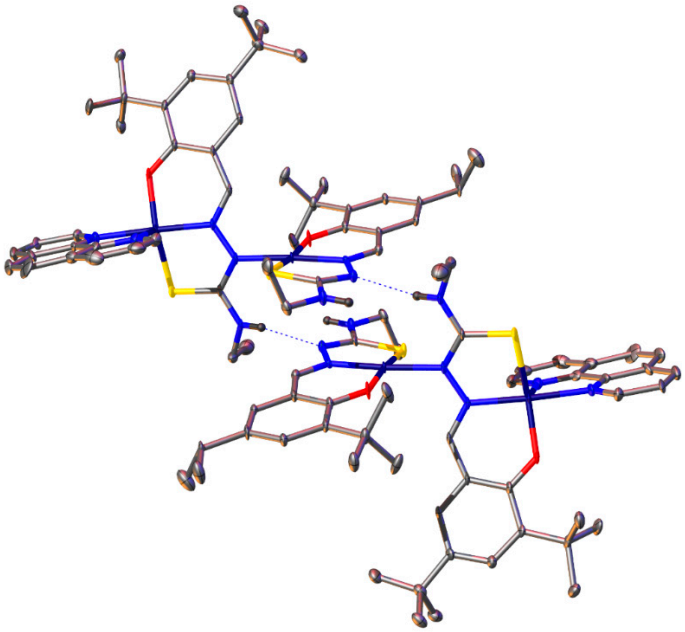

(b)

Figure 6. (a) Molecular structure of [Cu_2{(3,5-*t*-Bu_2)-sal4eT}$_2$(phen)] (**2**) and (b) illustration of dimerization of the dinuclear complex molecules.

The five-coordinate geometry at Cu(1) is similar to that described for the mononuclear ternary complex (**1**). The bidentate phen co-ligand adopts the axial-equatorial coordination mode. Consequently, the axial Cu–N_{phen} bond is tetragonally elongated, even longer than the Cu–S bond [Cu(1)–S(1) = 1.266(3) Å], causing asymmetric coordination of this co-ligand [Cu(1)–$N(4)_{eq}$ = 2.039(8) Å *vs.* Cu(1)–N(5) = 2.276(9) Å]. The copper(II) ion , Cu(1), resides 0.177(4) Å above the mean basal plane [N(1), S(1), O(1), N(4)] in the direction of the axial $N(5)_{phen}$ atom. Both copper(II) centres [Cu(1) and Cu(2)], regardless of the differences in the coordination geometries, have a $d_{x^2-y^2}$ ground state. The literature has witnessed a number of examples of crystallographically characterised dinuclear thiosemicarbazone complexes of copper(II), but these tend to have the same coordination geometry at the two metal centres [8–10,72]. To the best of our knowledge, the dinuclear complex [Cu_2{(3,5-*t*-Bu_2)-sal4eT}$_2$(phen)] (**2**) is one of only two of its kind. The other structurally characterised dinuclear thiosemicarbazone complex of copper(II) featuring two different coordination spheres is [Cu_2(sal4eT)$_2$(bipy)] (Scheme 1), reported as [$Cu_2(L^2)_2$(bipy)] [4]. Beyond the superficial similarities, there is a sharp distinction between the structures of [Cu_2{(3,5-*t*-Bu_2)-sal4eT}$_2$(phen)] (**2**) and [Cu_2(sal4eT)$_2$(bipy)] as regards the orientation of the ligands, intermolecular forces and the five-coordinate geometry at one of the two copper(II) centres. Unlike **2**, [Cu_2(sal4eT)$_2$(bipy)] exists as two independent complex molecules which are similar but not identical and the thiosemicarbazonate ligands are oriented (differently from **2**) such that *intramolecular hydrogen bonding* occurs between the phenolate oxygen atom bonded to the copper(II) ion in the distorted square planar geometry and the N^4–H group of the bridging quadridentate ligand. Moreover, the geometries of the five-coordinate copper(II) centres in the two molecules of [Cu_2(sal4eT)$_2$(bipy)] were reported as *distorted trigonal bipyramidal*. We have calculated their trigonality indices, τ_5 [74], to compare them with that of our dinuclear complex (**2**). For [Cu_2(sal4eT)$_2$(bipy)], the values of τ_5 are ~0.50 and ~0.51 (intermediate between square pyramidal and trigonal bipyramidal); in contrast, for **2**, τ_5 = 0.33, clearly pointing to greater distortion towards *square pyramidal*.

 doi:10.20944/preprints202312.1515.v1

2.7. X-Band ESR and UV-Visible Spectroscopic Characterisation

The X-band ESR spectrum of [Cu{(3,5-*t*-Bu$_2$)-sal4eT}(2,9-Me$_2$-phen)] (**1**) in frozen MeOH solution at 77 K, displayed in Figure 7, is axial. The ESR parameters $g_{\parallel}$ = 2.20, $g_{\perp}$ = 2.05, $A_{\parallel}$ = 19.3 mT and $A_{\perp}$ = 3 mT ($g_{\parallel} > g_{\perp} > 2.00$; $A_{\parallel} > A_{\perp}$) are consistent with the $d_{x^2-y^2}$ ground state [75,79–81]. Hence ESR spectroscopy demonstrated that the crystallographically determined distorted square pyramidal geometry at the metal centre is retained in solution. Figure 8 shows the electronic absorption spectra of H$_2$(3,5-*t*-Bu$_2$)-sal4eT, [Cu{(3,5-*t*-Bu$_2$)-sal4eT}(2,9-Me$_2$-phen)] (**1**) and [Cu$_2${(3,5-*t*-Bu$_2$)-sal4eT}$_2$(phen)] (**2**). The ligand is colourless; accordingly, its spectrum exhibits UV absorptions only. These hugely intense absorption bands are assignable to $\pi \rightarrow \pi^*$ (280–305 nm) and $n \rightarrow \pi^*$ (~338 nm) electronic transitions [4]. This pattern of UV absorptions is also observed in the spectra of **1** and **2**, albeit at somewhat higher energies. In the visible region of the electronic spectra of **1** and **2** are intense broad bands centred at 405 nm (ε_{max} ~ 17000 dm^3 mol^{-1} cm^{-1}) and 401 nm (ε_{max} ~ 20100 dm^3 mol^{-1} cm^{-1}), respectively, attributable to phenolate/thio-enolate-to-copper(II) charge-transfer electronic transitions [4]. Spin-allowed, but Laporte-forbidden, ligand-field transitions were observed as weak broad absorption bands at ~590 and ~570 nm for **1** and **2**, respectively. For distorted square-pyramidal copper(II) complexes, such *d-d* electronic transitions have been assigned previously as $d_{xz}, d_{yz} \rightarrow d_{x^2-y^2}$ in nature [79].

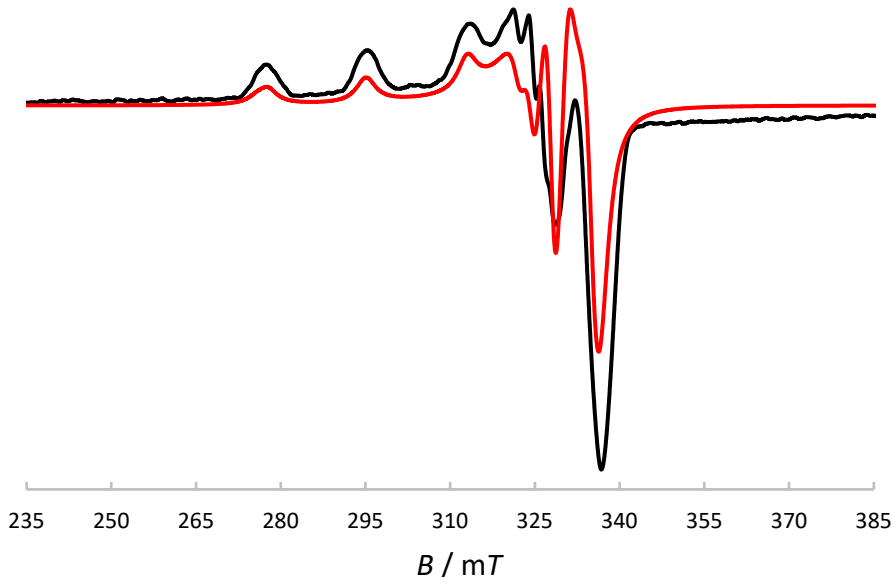

Figure 7. X-band ESR spectrum of [Cu{(3,5-*t*-Bu$_2$)-sal4eT}(2,9-Me$_2$-phen)] (**1**) recorded in frozen MeOH solution at 77 K (ν = 9.3641 GHz).

Preprints (www.preprints.org) | NOT PEER-REVIEWED | Posted: 20 December 2023 doi:10.20944/preprints202312.1515.v1

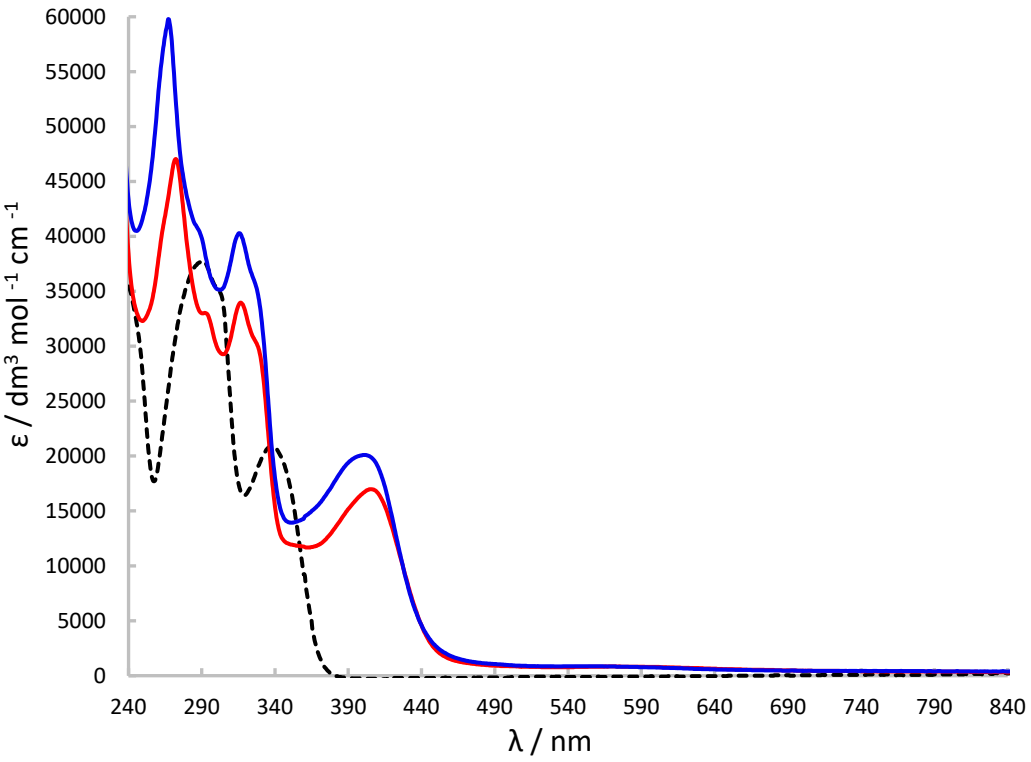

Figure 8. Electronic absorption spectra of H_2(3,5-*t*-Bu_2)-sal4eT, [Cu{(3,5-*t*-Bu_2)-sal4eT}(2,9-Me_2-phen)] (**1**) and [Cu_2{(3,5-*t*-Bu_2)-sal4eT}$_2$(phen)] (**2**) in MeOH.

2.8. In Vitro Cytotoxicity of the Thiosemicarbazone Ligand and the Ternary Copper(II) Complexes

The antiproliferative activity of H_2(3,5-*t*-Bu_2)-sal4eT, [Cu{(3,5-*t*-Bu_2)-sal4eT}(2,9-Me_2-phen)] (**1**) and [Cu_2{(3,5-*t*-Bu_2)-sal4eT}$_2$(phen)] (**2**) was investigated in two cancer cell lines, namely human cervical carcinoma (HeLa) and human breast adenocarcinoma (MCF-7) using the MTT cell viability assay [MTT = 3-(4,5-dimethylthiazol-2-yl)-2,5-diphenyltetrazolium bromide]. The values of the 50% inhibitory concentrations (IC_{50}) of these substances together with the positive controls (docetaxel and paclitaxel) were determined as exemplified for complexes **1** and **2** in the HeLa and MCF-7 cancer cells, respectively (Figure 9). The *in vitro* antiproliferative potential of each substance was tested within the 0.01–100-μ*M* range of concentrations; the results of these cytotoxicity measurements are presented in Table 4. IC_{50} values for cisplatin were obtained from the literature [82,83].

In striking contrast to the marked potent and selective antiproliferative activity of naphthol- and pyridyl-based thiosemicarbazones [11,12], together with their corresponding metal complexes, against tumour cells, the phenolic thiosemicarbazone H_2(3,5-*t*-Bu_2)-sal4eT is nontoxic towards both cancer cells in this investigation. However, as is often the case with hydrazones, complexation with metal ions induces phamarcological activity as can be seen from Table 4. Intriguingly, complex **1** exhibits selective potency towards the Hela cancer cells over the MCF-7 cancer cells. Conversely, the antiproliferative activity of complex **2** is specific towards MCF-7. Although this behaviour has only been observed from tests carried out *in vitro*, these results show that these copper(II) thiosemicarbazone complexes have potential applications as metallo-drugs in targeted cancer treatment.

 doi:10.20944/preprints202312.1515.v1

Table 4. Cytotoxicity evaluation of H(3,5-*t*-Bu$_2$)-sal4eT, **1** and **2** by MTT assay in cancer cell lines over a 24-hour incubation period.

	IC_{50} / μ*M*	
Compound	**HeLa**	**MCF-7**
H(3,5-*t*-Bu$_2$)-sal4eT	>100	>100
[Cu{3,5-*t*-Bu$_2$)-sal4eT}(2,9-Me$_2$-phen)] (**1**)	1.35 ± 0.11	>100
[Cu$_2$\{3,5-*t*-Bu$_2$)-sal4eT\}$_2$(phen)] (**2**)	>100	0.73 ± 0.06
Docetaxel	60.70 ± 5.13	92.54 ± 7.99
Paclitaxel	15.84±1.28	>100
Cisplatin	13.28 ± 3.84 [82]	13.36 ± 1.25 [83]

Their selectivity over non-cancerous cells such as the human breast epithelial cell line (MCF-10A), have yet to be determined. It is noteworthy that in vitro complexes **1** and **2** are more efficacious as antiproliferative agents than cisplatin. Moreover, cisplatin lacks the cancer-specificity which these complexes possess. They also exhibit higher potent anticancer activity than the standards. Although the study of the mode of action of complexes **1** and **2** as anticancer agents is beyond the scope of this work, it has been amply demonstrated previously for a diverse range of copper(II) complexes, including those of thiosemicarbazones, that the potentials of the Cu^{II}/Cu^{I} redox couple [8,15,18,20,30] lie within the biologically accessible redox potential window leading to the generation of reactive oxygen species (ROS) which cause apoptotic cell death.

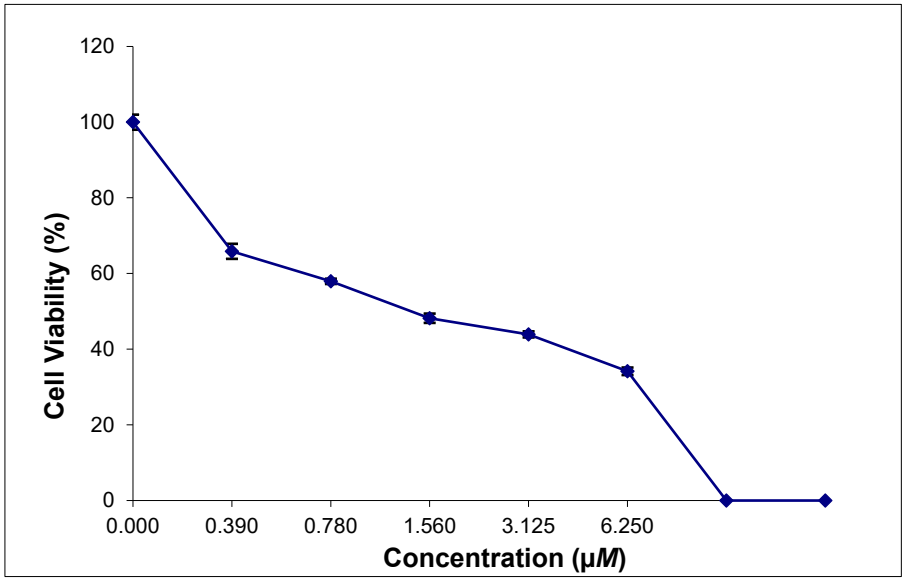

(a)

Preprints (www.preprints.org) | NOT PEER-REVIEWED | Posted: 20 December 2023 doi:10.20944/preprints202312.1515.v1

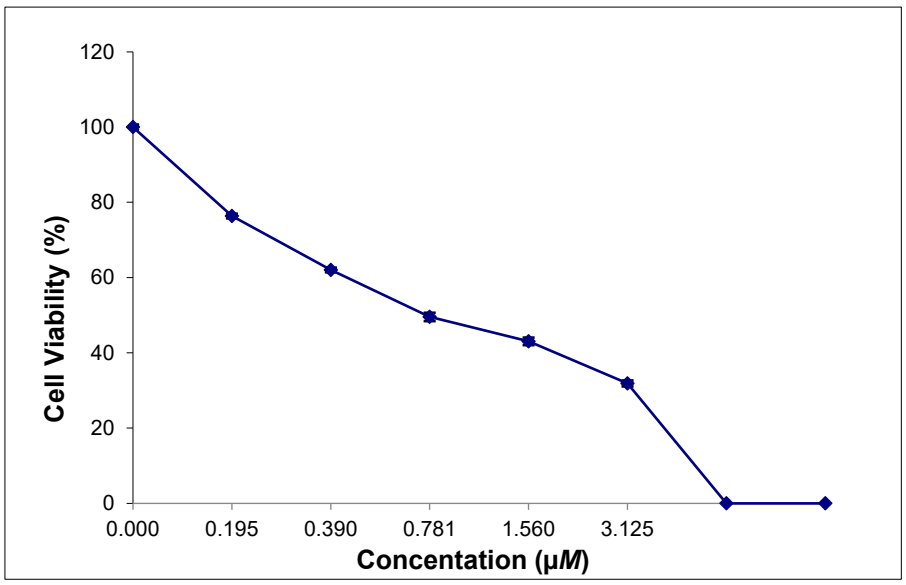

(b)

Figure 9. Cytotoxicity of [Cu{(3,5-*t*-Bu$_2$)-sal4eT}(2,9-Me$_2$-phen)] (**1**) towards HeLa cells (a) and [Cu$_2$\{(3,5-*t*-Bu$_2$)-sal4eT\}$_2$(phen)] (**2**) towards MCF-7 cells (b).

3. Conclusion

The thiosemicarbazone H$_2$(3,5-*t*-Bu$_2$)-sal4eT and its ternary copper(II) complexes [Cu{(3,5-*t*-Bu$_2$)-sal4eT}(2,9-Me$_2$-phen)] (**1**) and [Cu$_2$\{(3,5-*t*-Bu$_2$)-sal4eT\}$_2$(phen)] (**2**) have been synthesised and their chemical identities ascertained by microanalyses, mass spectrometry and vibrational spectroscopy. Definitive evidence for their 3-D structures was provided by single-crystal X-ray analyses. As is commonly the case with phenolic thiosemicarbazones, this ligand was isolated as the thio-keto (thione) tautomer and in the *E*-configuration with respect to the Schiff-base imine bond. ^{1}H-NMR spectroscopy showed that this isomeric form is maintained in solution. The X-ray structures of complexes [Cu{(3,5-*t*-Bu$_2$)-sal4eT}(2,9-Me$_2$-phen)] (**1**) and [Cu$_2$\{(3,5-*t*-Bu$_2$)-sal4eT\}$_2$(phen)] (**2**) show that the thiosemicarbazone underwent base/metal-assisted tautomerization upon coordination to copper(II); moreover, this ligand also demonstrated coordination versatility in that in complex **2** it employed two different denticities, namely tridentate and quadridentate. The planarity and rigidity of the thiosemicarbazonate ligand and the co-ligand 2,9-dimethyl-1,10-phenanthroline imposed a distorted square-pyramidal geometry at the metal centre of complex **1** (τ = 0.14) whereby the donor atoms of the tridentate primary ligand are arranged meridionally whereas the bidentate co-ligand adopts an axial-equatorial coordination mode. As always observed in X-ray structures of this type of ternary copper(II) complexes, there is considerable elongation of the axial coordinate bond in conformity with the tetragonal distortion. The ESR spectrum of **1** in frozen solution is axial ($g_\parallel > g_\perp >$ 2.00; $A_\parallel > A_\perp$) and indicative of half occupancy of the $d_{x^2-y^2}$ orbital. The dinuclear complex (**2**) exhibits different coordination geometries at the copper(II) centres, namely distorted square planar and distorted square pyramidal. Such dinuclear ternary copper(II) complexes are few and far between. Intriguingly, the cytotoxicity activities of [Cu{(3,5-*t*-Bu$_2$)-sal4eT}(2,9-Me$_2$-phen)] and [Cu$_2$\{(3,5-*t*-Bu$_2$)-sal4eT\}$_2$(phen)] in the HeLa and MCF-7 cancer cell lines are vastly different. Whereas the former is highly antiproliferative against HeLa cancer cells but non-toxic towards MCF-7 cancer cells, the converse is true for the latter. Such selective cytotoxicity of **1** and **2** towards these cancer cells is not shown by cisplatin.

 doi:10.20944/preprints202312.1515.v1

4. Experimental

4.1. Materials and Physical Techniques

All pertinent chemicals, reagents and solvents (HPLC/AR-grade) were purchased from Sigma-Aldrich and used as received. Microanalyses (CHN) were performed on a EuroVector elemental analyser. ESI mass spectra were measured with an Agilent 6460 Triple Quadrupole mass spectrometer using MeOH as a matrix. Electrical conductivities of the complexes were determined with a JENWAY 4520 conductivity meter at room temperature using freshly prepared solutions (1 m*M*) in MeOH. FT-IR spectra were recorded on a Perkin-Elmer spectrophotometer (4000–400 cm^{-1}) with the samples compressed as KBr discs using a Specac press. ^{1}H NMR spectroscopic measurements were carried out at room temperature in DMSO-d_6 on a Bruker ASCEN 700 spectrometer operating at radiofrequencies of 700 MHz, respectively; the chemical shifts are referenced to TMS as an internal standard (δ = 0). X-band ESR spectra of the copper(II) complexes were recorded on a Bruker ELEXSYS E580X FT CW spectrometer (ν ~ 9.4 GHz). Electronic absorption spectra were measured with a Shimadzu 2450 UV-visible spectrophotometer (190–1000 nm) using freshly prepared solutions. Magnetic susceptibility measurements were carried out at room temperature using a Sherwood Scientific magnetic susceptibility balance. The magnetic data were corrected for diamagnetism using Pascal's constants the usual way ($x_{para} = x_{meas} - x_{dia}$). Single-crystal X-ray structure determinations were carried out on a Bruker APEX-II CCD area-detector diffractometer or a Bruker D8 Venture CMOS Photon 100 diffractometer. The crystals were mounted in fomblin oil and cooled in a stream of cold N_2. Data were corrected for absorption using empirical methods (SADABS) [84] based upon symmetry equivalent reflections combined with measurements at different azimuthal angles [85]. The crystal structures were solved and refined against F^2 values using ShelXT [86] for solution and ShelXL [87] for refinement (using least squares minimisation) accessed via the Olex2 programme [88].

4.2. Synthesis of H_2(3,5-t-Bu_2)-sal4eT

A sample of 3,5-di-*tert*-butylsalicylaldehyde (2.3433 g, 10.00 mmol) was dissolved in EtOH (30 mL). Separately, 4-ethyl-3-thiosemicarbazide (1.1919 g, 10.00 mmol) was dissolved in EtOH (30 mL). Then these two solutions were mixed together and the resultant solution heated under reflux over a period of three hours. On standing at room temperature for four days, the solution deposited shiny colourless crystals. This product was filtered off on the Büchner funnel, washed with ice-cold EtOH and dried in air (yield: 2.2419 g, 66.82%). Characterization: calcd for $C_{18}H_{29}N_3OS$ (M = 335.50 g/mol): C, 64.44%; H, 8.71%; N, 12.52%. Found: C, 64.17%; H, 8.55%; N, 12.63%; m.p. 218–219^{0}C.

*4.3. Synthesis of [Cu{(3,5-t-Bu_2)-sal4eT}(2,9-Me_2-phen)] (**1**)*

To a hot solution of H_2(3,5-t-Bu_2)-sal4eT (0.1342 g, 0.40 mmol) in MeOH (30 mL) were added $Cu(OAc)_2{\cdot}H_2O$ (0.0799 g, 0.40 mmol) and 2,9-dimethyl-1,10-phenanthroline (0.0833 g, 0.40 mmol) consecutively with vigorous swirling. The resultant reaction mixture was heated under reflux for 15 minutes and then filtered and kept at room temperature. Upon slow solvent evaporation from the solution under ambient conditions over a period of one week, shiny black blocks were formed. This crystalline product was isolated by decantation of the mother liquor, washed with ice-cold EtOH and then left to dry in air (yield: 0.2160 g, 89.23%). Characterization: calcd for $C_{32}H_{39}CuN_5OS$ (M = 605.28 g/mol): C, 63.50%; H, 6.49%; N, 11.57%. Found: C, 63.37%; H, 6.50%; N, 11.58%; m.p. 248–249^{0}C.

*4.4. Synthesis of [Cu_2}(3,5-t-Bu_2)-sal4eT}$_2$(phen)] (**2**)*

This complex was synthesised as described for complex **1** above except that 1,10-phenanthroline monohydrate (0.0793 g, 0.4000 mmol) was used as a co-ligand instead of 2,9-dimethyl-1,10-phenanthroline. The resultant dark green solution was heated under reflux for 15 minutes and then filtered. Large shiny black crystals were obtained from the solution after one week of standing at room temperature. After removal of the supernatant, the crystals were washed with ice-cold EtOH

and kept in air (yield: 0.1576 g, 80.86%). Characterization: calcd for $C_{48}H_{62}Cu_2N_8O_2S_2$ (MM = 974.25 g/mol): C, 59.17%; H, 6.41%; N, 11.50%. Found: C, 59.53%; H, 6.29%; N, 11.38%; m.p. 222–224^{0}C.

4.5. Investigation of Anticancer Activity

4.5.1. Cell Lines and Cell Culture

Two cancerous cell lines, namely MCF-7 (human breast adenocarcinoma) and HeLa (human cervical carcinoma) were obtained from the Pasteur Institute (Tehran, Iran). The cells were cultured in RPMI-1640 medium (Sigma) supplemented with 10% heat-inactivated foetal bovine serum (FBS; Gibco, USA), penicillin (100 U/mL) and streptomycin (100 µg/mL) (Roche, Germany) at 37°C in a humidified incubator with 5% CO_2.

4.5.2. Cytotoxicity Evaluation by the MTT Assay

All the final compounds were investigated for their antiproliferative potential at 0.01–100 µM concentrations. Three controls were prepared within each 96-well plate: a solvent [dimethyl sulfoxide (DMSO)] control and a positive controls (paclitaxel & Docetaxel). Briefly, appropriate cells were seeded in 96-well plates (Nunc, Roskilde, Denmark) at a density of 10 000 viable cells per well and incubated for 24 h to allow for cell attachment. Solutions of the compounds were prepared by serial dilution from the stock solution and added to each well. Cells were then incubated with the compounds for another 48 h. The response of cells to compounds was evaluated by determining the cell survival using 3-(4,5-dimethylthiazoyl- 2-yl) 2,5-diphenyl tetrazolium bromide (MTT, Carl Roth, Karlsruhe, Germany). At first, cells were washed with phosphate buffered saline (PBS) and then 20 µL of the MTT reagent (5 mg/mL) in PBS was added to each well. After 4 h of incubation at 37°C, the medium was discarded, DMSO (100 µL) was added to each well and the plates were vigorously shaken to dissolve the purple tetrazolium crystals in DMSO. The absorbance of each well was measured using a plate reader (Anthous 2020; Austria) at a test wavelength of 550 nm against a standard reference solution at 690 nm. Assays were performed in triplicate in three independent experiments, and the concentration required for 50% inhibition of cell viability (IC_{50}) was determined from a plot of the percentage cytotoxicity versus the concentration on a logarithmic graph.

Supplementary Materials: The following supporting information can be downloaded at the website of this paper posted on Preprints.org.

Conflicts of Interest: The authors declare no conflict of interest.

References

1. Lobana, T. S.; Sharma, R; Bawa, G.; Khanna, S. Bonding and structure trends of thiosemicarbazone derivatives of metals – an overview. *Coord. Chem. Rev.* **2009**, *253*, 977–1055.
2. Papathanasis, L.; Demertzis, M. A.; Yadav, P. N.; Kovala-Demertzi, D.; Prentjas, C.; Castiñeiras, A.; Skoulika, S.; West D. X. Palladium(II) and platinum(II) complexes of 2-hydroxyacetophenone *N*(4)-ethylthiosemicarbazone – crystal structure and description of bonding properties. *Inorg. Chim. Acta* **2004**, *357*, 4113–4120.
3. Zhang, Z.; Gou, Y.; Wang, J.; Yang, K.; Qi, J.; Zhou, Z.; Liang, S.; Liang, H.; Yang, F. Four copper(II) compounds synthesized by anion regulation: structure, anticancer function and anticancer mechanism. *Eur. J. Med. Chem*, **2016**, *121*, 399–409.
4. Lobana, T.S.; Kumari, P.; Bitcher, R.; Jasinski, J.P.; Golen, J.A. Metal derivatives of thiosemicarbazones: crystal and molecular structures of mono- and dinuclear copper(II) complexes with N^1-substituted salicylaldehyde rhiosemicarbazones. *Z. Anorg. Allg Chem.* **2012**, *638*, 1861–1867.
5. Lobana, T. S.; Kumari, P.; Castiñeiras, A.; Butcher, R. J. The effect of C-2 substituents of salicyladehyde-based thiosemicarbazones on the synthesis, spectroscopy, structures, and fluorescence of nickel(II) complexes. *Eur. J. Inorg. Chem.* **2013**, 3557–3566.

6. Kumari, P.; Lobana, S. T; Butcher, R. J. Castiñeiras, A.; Zeller, M. The effect of substituents at C^2/N^1 atoms of salicylaldehyde and 2-hydroxyacetophenone-based thiosemicarbazones on the nature of nickel(II) complexes with 1,10-phenanthroline and terpyridine as co-ligands. *Inorg. Chim. Acta* **2018**, *482*, 268–274.
7. Pereiras-Gabián, G.; Vázquez-López, M.; Abram, U. Dimeric rhenium(I) carbonyl complexes with thiosemicarbazone backbone. *Z. Anorg. Allg. Chem.* **2004**, *630*, 1665–1670.
8. Qi, J.; Yao, Q.; Tian, L.; Wang, Y. Piperidylthiosemicarbazones Cu(II) complexes with a high anticancer activity by catalysing hydrogen peroxide to degrade DNA and promote apoptosis. *Eur. J. Med. Chem.* **2018**, *158*, 853–862.
9. Qi, J.; Liang, S.; Gou, Y.; Zhang, Z.; Zhou, Z.; Yang, F.; Liang, H. Synthesis of four binuclear copper(II) complexes: structure, anticancer properties and anticancer mechanism. *Eur. J. Med. Chem.* **2015**, *96*, 360–368.
10. Duan, C.-Y.; Wu, B.-M.; Mak, T. C. W.; Synthesis and structural characterization of new quadridentate N_3S-compound di-2-pyridyl ketone thiosemicarbazone and its binuclear copper(II) complexes. *J. Chem. Soc., Dalton Trans.* **1996**, 3485–3490.
11. Lovejoy, D. B.; Richardson, D. R. Novel "hybrid" iron chelators derived from aroylhydrazones and thiosemicarbazones demonstrate selective antiproliferative activity against tumor cells. *Blood*, **2002**, 100, 666–676.
12. Yuan, J.; Lovejoy, D. B.; Richardson, D. R. Novel di-pyridyl-derived iron chelators with marked and selective antitumor activity: in vitro and in vivo assessment. *Blood*, **2004**, *104*, 1450–1458.
13. Richardson, D. R.; Sharpe, P. C.; Lovejoy, D. B.; Senaratne, D.; Kalinowski, D. S.; Islam, M.; Bernhardt, P. V. Dipyridyl thiosemicarbazone chelators with potent and selective antitumour activity form iron complexes with redox activity. *J. Med. Chem.* **2006**, *49*, 6510–6521.
14. Kalinowski, D. S.; Yu, Y.; Sharpe, P. C.; Islam, M.; Liao, Y.-T.; Lovejoy, D. B.; Kumar, N.; Bernhardt, P. V.; Richardson, D. R. Design, synthesis, and characterization of novel iron chelators: structure-activity relationships of the 2-benzoylpyridine thiosemicarbazone series and their 3-nitrobenzoyl analogues as potent antitumor agents. *J. Med. Chem.* **2007**, *50*, 3716–3729.
15. Richardson, D. R.; Kalinowski, D. S.; Richardson, V.; Sharpe, P. C.; Lovejoy, D. B.; Islam, M.; Bernhardt, P. V. 2-Acetylpyridine thiosemicarbazones are potent iron chelators and antiproliferative agents: redox activity, iron complexation and characterization of their antitumor activity. *J. Med. Chem*. **2009**, *52*, 1459–1470.
16. Jansson, P. J.; Sharpe, P. C.; Bernhardt, P. V.; Richardson, D. R. Novel thiosemicarbazones of the ApT and DpT series and their copper complexes: identification of pronounced redox activity and characterization of their antitumor activity. *J. Med. Chem.* **2010**, *53*, 5759–5769.
17. Stefani, C.; Punnia-Moorthy, G.; Lovejoy, D. B.; Jansson, P. J.; Kalinowski, D. S.; Sharpe, P. C.; Bernhardt, P. V.; Richardson, D. R. Halogenated 2′-benzoylpyridine thiosemicarbazone (XBpT) chelators with potent and selective anti-neoplastic activity: relationship to intracellular redox activity. *J. Med. Chem.* **2011**, *54*, 6936–6948.
18. Lovejoy, D. B.; Sharp, D. M.; Seebacher,N.; Obeidy, P.; Prichard, T.; Stefani, C.; Basha, M. T.; Sharpe, P. C.; Jansson, P. J.; Kalinowski, D. S.; Bernhardt, P. V.; Richardson, D. R. Novel second-generation di-2-pyridylketone thiosemicarbazones show synergism with standard chemotherapeutics and demonstrate potent activity against lung cancer xenografts after oral and intravenous administration in vivo. *J. Med. Chem.* **2012**, *55*, 7230–7244.
19. Stefani, C.; Jansson, P. J.; Gutierrez, E.; Bernhardt, P. V.; Richardson, D. R.; Kalinowski, D. S. Alkyl substituted 2′-benzoylpyridine thiosemicarbazone chelators with potent and selective anti-neoplastic activity: novel ligands that limit methemoglobin formation. *J. Med. Chem.* **2013**, *56*, 357–370.
20. Ohui, K.; Afanasenko, E.; Bacher, F.; Ting, R. L. X.; Zafar, A.; Blanco-Cabra, N.; Torrents, E.; Dömötör, O.; May, N. V.; Darvasiova, D.; Enyedy, E. A.; Popović-Bijelić, A.; Reynisson, J.; Rapta, P.; Babak, M. V.; Pastorin, G.; Arion, V. B. New water-soluble copper(II) complexes with morpholine-thiosemicarbazone hybrids: insights into the anticancer and antibacterial mode of action. *J. Med. Chem.* **2019**, *62*, 512–530.
21. Wang, J. Zhang, Z.-M.; Li, M.-X. Synthesis, characterization, and biological activity of cadmium(II) and antimony(III) complexes based on 2-acetylpyrazine thiosemicarbazones. *Inorg. Chim. Acta* **2022**, *530*, 120671.
22. Savir, S.; Liew, J. W. K.; Vythilingam, I.; Lim, Y. A. L.; Tan, C. H.; Sim, K. S.; Lee, V. S.; Maah, M. J.; Tan, K. W. Nickel(II) complexes with plyhydroxybenzaldehyde and O,N,S tridentate thiosemicarbazone ligands:

synthesis, cytotoxicity, antimalarial activity, and molecular docking studies. *J. Mol. Struct.* **2021**, *1242*, 130815.

23. Rodríguez-Argüelles, M. C.; López-Silva, E. C.; Sanmartín J.; Pelagatti, P.; Zani, F. Copper complexes of imidazole-2-, pyrrole-2- and indol-3-carbaldehyde thiosemicarbazones: inhibitory activity against fungi and bacteria. *J. Inorg. Biochem.* **2005**, *99*, 2231–2239.
24. Genova, P.; Varadinova, T.; Matesanz, A. I.; Marinova, D.; Souza, P. Toxic effects of bis(thiosemicarbazone) compounds and its palladium(II) complexes on herpes simplex virus growth. *Toxicol. Appl. Pharmacol.* **2004**, *197*, 107–112.
25. Karaküçük-İyidoğan, A.; Taşdemir, D.; Oruç-Emre, E. E.; Balzarini, J. Novel platinum(II) and palladium(II) complexes of thiosemicarbazones derived from 5-substitutedthiophene-2-carbaldehydes and their antiviral and cytotoxicity activities. *Eur. J. Med. Chem.* **2011**, *46*, 5616–5624.
26. Bajaj, K.; Buchanan, R. M.; Grapperhaus, C. A. Antifungal activity of thiosemicarbazones, bis(thiosemicarbazones), and their metal complexes. *J. Inorg. Biochem.* **2021**, *225*, 111620.
27. Khanye, S. D.; Smith, G. S.; Lategan, C.; Smith, P. J.; Gut, J.; Rosenthal, P. J.; Chibale, K. Synthesis and in vitro evaluation of gold(I) thiosemicarbazone complexes for antimalarial activity. *J. Inorg. Biochem.* **2010**, *104*, 1079–1083.
28. Kang, S.; Shiota, Y.; Kariyazaki, A.; Kanegawa, S.; Yoshizawa, K.; Sato, O. Heterometallic Fe^{III}/K coordination polymer with a wide thermal hysteretic spin transition at room temperature. *Chem. Eur. J.* **2016**, *22*, 532–538.
29. Kovala-Demertzi, D.; Yadav, P.N.; Demertzis, M.A.; Jasiski, J.P.; Andreadaki, F.J.; Kostas, I.D. First use of a palladium complex with a thiosemicarbazone ligand as catalyst precursor for the Heck reaction. *Tetrahedron Lett.* **2004**, *45*, 2923–2926.
30. Jungwirth, U.; Kowol, C.R.; Keppler, B.K.; Hartinger, C.G.; Berger, W.; Heffeter, P. Anticancer Activity of Metal Complexes: Involvement of Redox Processes. *Antioxid. Redox Signal.* **2011**, *15*, 1085–1127.
31. Mohan, B.; Chaudhary. M.; Synthesis, crystal structure, computational study and anti-virus effect of mixed ligand copper(II) complex with ONS donor Schiff base and 1,10-phenanthroline. *J. Mol. Struct.*, **2021**, 1246, 131246.
32. Ambalavanan, P.; Palani, K.; Ponnuswamy, M.N. Crystal structure of [1-(2-phenyloxyN[N-cyclohexylthiouryl)] ethylamine-(1,10-phenanthrolinyl)]copper(II). *Cryst. Res. Technol.* **2002**, *37*, 1249–1254.
33. Naik, A.D.; Reddy, P.A.N.; Nethaji, M.; Chakravarty, A.R. Ternary copper(II) complexes of thiosemicarbazones and heterocyclic bases showing N_3OS coordination as models for the type-2 centers of copper monooxygenases. *Inorg. Chim. Acta* **2003**, 349, 149–158.
34. Thomas A.M.; Naik, A.D.; Nethaji, M.; Chakravarty, A.R. Synthesis, crystal structure and photo-induced DNA cleavage activity of ternary copper(II)-thiosemicarbazone complexes having heterocyclic bases. *Inorg. Chim. Acta* **2004**, *357*, 2315–2323.
35. Lobana, T.S.; Indoria, S.; Jassal, A.K.; Kaur, H.; Arora, D.S.; Jasinski, J.P. Synthesis, structures, spectroscopy and antimicrobial properties of complexes of copper(II) with salicylaldehyde N-substituted thiosemicarbazones and 2,2′-bipyridine or 1,10-phenanthroline. *Eur. J. Med. Chem.* **2014**, *76*, 145–154.
36. Indoria, S.; Lobana, T.S.; Kauer, H.; Arora, D.S.; Randhawa, B.S.; Jassal, A.K.; Jasinski, J.P. Synthesis and structures of 5-methoxysalicyladehyde thiosemicarbazonates of copper(II): molecular spectroscopy, ESI-mass studies and antimicrobial activity. *Polyhedron*, **2016**, *107*, 9–18.
37. Lobana, T.S.; Indoria, S.; Sood, S.; Arora, D.S.; Randhawa, B.S.; Garcia-Santos, I.; Smolinski, V.A.; Jasinski, J.P. Synthesis of 5-nitrosalicylaldehyde-N-substituted thiosemicarbazonates of copper(II): molecular structures, spectroscopy, ESI-mass studies and antimicrobial activity. *Inorg. Chim Acta* **2017**, *46*, 248–260.
38. Ainscough, E.W.; Brodie, A.M.; Ranford, J.D.; Waters, J.M. Reaction of nitrogen and sulphur donor ligands with the antitumour complex [{CuL($MeCO_2$)}$_2$] (HL = 2-formylpyridine thiosemicarbazone) and the single-crystal X-ray structureof [CuL(bipy)]ClO_4 (bipy = 2,2′-bipyridine). *J. Chem. Soc., Dalton Trans.* **1991**, 1737–1742.
39. Kartikeyan, R.; Murugan, D.; Ajaykamal, T.; Varadhan, M.; Rangasamy, L.; Velusamy, M.; Palaniandavar, M.; Rajendiran, V. Mixed ligand copper(II)-diimine complexes of 2-formylpyridine-N^4-phenylthiosemicarbazone: diimine co-ligands tune the *in vitro* nanomolar cytotoxicity. *Dalton Trans.* **2023**, *52*, 9148–9169.

40. Sreeja, P.B.; Kurup, M.R.P.; Kishore, A.; Jasmin, C. Spectral characterization, X-ray structure and biological investigations of copper(II) ternary complexes of 2-hydroxyacetophenone 4-hydroxybenzoic acid hydrazone and heterocyclic bases, *Polyhedron* **2004**, *23*, 575–581.
41. Reddy, P.A.N.; Santra, B.K.; Nethji, M.; Chakravarty, A.R. Metal-assisted light-induced DNA cleavage activity of 2-(methylthio)phenylsalicyladimine Shiff base copper(II) complexes having planar heterocyclic bases. *J. Inorg, Biochem.* **2004**, *98*, 377–386.
42. Reddy, P.R.; Shilpa, A.; Raju, N.; Raghavaiah, P. Synthesis, structure, DNA binding and cleavage properties of ternary amino acid Schiff base-phen/bipy Cu(II) complexes. *J. Inorg. Biochem.* **2011,** *105*, 1603–1612.
43. Li. A.; Liu, Y.-H.; Yuan, L.-Z.; Ma, Z.-Y.; Zhao, C.-L.; Xie, C.-Z.; Bao, W.-G.; Xu, J.-Y. Association of structural modifications with bioactivity in three new copper(II) complexes of Schiff base ligands derived from 5-chlorosalicylaldehyde and amino acids. *J. Inorg. Biochem*. **2015**, *146*, 52–60.
44. Rajendiran, .; karthik, R.; Palaniandavar, M.; Stoeckli-Evans, H.; Periasamy, V.S.; Akbarsha, M.A.; Srinag, B.S.; Krishnamurthy, H. Mixed-ligand copper(II)-phenolate complexes: effect of coligand on enhanced DNA and protein binding, DNA cleavage, and anticancer activity. *Inorg. Chem.* **2007**, *46*, 8208–8221.
45. Reddy, P.A.N.; Nethaji, M.; Chakravarty, A.R.; Synthesis, crystal structures and properties of ternary copper(II) complexes having 2,2′-bipyridine and amino acid salicylaldiminates as models for the type-2 sites in copper oxidases. *Inorg. Chim. Acta*, **2002**, 337, 450–458.
46. Mathew, N.; Sithambaresan, M.; Kurup, M.R.P. Spectral studies of copper(II) complexes of tridentate acylhdrazone ligands with heterocyclic compounds as coligands: X-ray crystal structure of one acylhydrazone copper(II) complex. *Spectrochim. Acta Part A,* **2011**, *79*, 1154–1161.
47. Koh, L.L.; Ranford, J.O.; Robinson, W.T.; Svensson, J.O.; Tan, A.L.C.; Wu, D. Model for the reduced Schiff base intermediate between amino acids and pyridoxal: copper(II) complexes of *N*-(2-hdroxybenzyl)amino acids with nonpolar side chains and the crystal structures of [Cu(*N*-(2-hydroxybenzyl)-D,L-alanine)(phen·H_2O and [Cu(*N*-(2-hydroxybenzyl)-D,L-alanine)(imidazole)]. *Inorg. Chem.* **1996**, *35*, 6466–6472.
48. Bernal, M.; García-Vázquez, J.A.; Romero, J.; Gómez, C.; Durán, M. L.; Sousa, A.; Sousa-Pedrares, A.; Rose, D.J.; Maresca, K.P.; Zubieta, J. Electrochemical synthesis of cobalt, nickel, zinc and cadmium complexes with *N*[(2-hydroxyphenyl)methylidine]-*N´*-tosylbenzene-1,2-diamine. The crystal structures of {1,10-phenanthroline)[*N*-2-oxophenyl)methylidine]-*N*-tosylbenzene-1,2-diaminato}nickel(II) and {1,10-phenanthroline)[*N*-2-oxophenyl)methylidine]-*N´*-tosylbenzene-1,2-diaminato}copper(II). *Inorg. Chim. Acta* **1999**, *295*, 39–47.
49. Wang, M.-Z.; Meng, Z.-X; Liu, B.L.; Cai, G.-L.; Zhang, C.-L.; Wang, X.-Y. Novel tumor chemotherapeutic agents and tumor radio-imaging agents: potential tumor pharmaceuticals of ternary copper(II) complexes. *Inorg. Chem. Commun.* **2005,** *8* 368–371.
50. Reddy, P.A.N.; Nethaji, M.; Chakravarty, A.R. Hydrolytic cleavage of DNA by ternary amino acid Schiff base copper(II) complexes having planar heterocyclic ligands. *Eur. J. Inorg. Chem.* **2004**, 1440–1446.
51. Dong, J.; Li, L.; Liu, G.; Xu, T.; Wang, D. Synthesis, crystal structure and DNA-binding properties of a new copper(II) complex with L-valine Schiff base and 1,10-phenanthroline. *J. Mol. Struct.* **2011**, *986*, 57–63.
52. Labisbal, E.; Garcia-Vazquez, Romero, J.; Picos, S.; Sousa, A.; Castiñeiras, A.; Maichle-Mössmer. Electrochemical synthesis and structural characterization of nickel(II) and copper(II) complexes of tridentate Schiff bases: molecular structure and the five-coordinated copper(II) complex: 1,10-phenanthroline {2-[2-oxyphenyl)iminomethyl]phenolato}copper(II). *Polyhedron* **1995**, *14*, 663–670.
53. Sharma, M.; Ganeshpandian, M.; Majumder, M.; Tamilarasan, A.; Sharma, M.; Mukhopadhyay, R.; Islam, N.S.; Palaniandavar, M. Octahedral copper(II)-diimine complexes of triethylenetetramine: effect of stereochemical fluxionality and ligand hydrophobicity on Cu^{II}/Cu^{I} redox, DNA binding and cleavage, cytotoxicity and apoptosis-inducing ability. *Dalton Trans.* **2020**, *49,* 8282–8297.
54. Ng, C.H.; Kong, K.C.; Von,S.T.; Balraj, P.; Jensen, P.; Thirthagiri, E.; Hamada, H.; Chikira, M. Synthesis, characterization, DNA-binding stuídy and anticancer properties of ternary metal(II) complexes of edda and an intercalating ligand. *Dalton Trans.* **2008**, 447–454.
55. Selvakumar, B.; Rajendiran, V.; Maheswari, P.U.; Stoeckli-Evans, H.; Palaniandavar, M. Structures, spectra, and DNA-binding properties of mixed ligand copper(II) complexes of iminodiacetic acid: the novel role of diamine co-ligands on DNA conformation and hydrolytic and oxidative double strand DNA cleavage. *J. Inorg. Biochem.* **2006**, *100*, 316–330.

56. Yang, C.-T.; Moubaraki, B.; Murray, K.S.; Vittal, J.J. Synthesis, characterization and properties of ternary copper(II) complexes containing reduced Schiff base *N*-(2-hdroxybenzyl)-amino acids and 1,10-phenanthroline. *Dalton Trans.* **2003**, 880–890.
57. Yang, C.T.; Moubaraki, B.; Murray, K.S.; Ranford, J.D.; Vittal, J.J. Interconversion of a monomer and two coordination polymers of a copper(II)-reduced Schiff base ligand-1,10-phenanthroline complex based on hydrogen- and coordinative-bonding. *Inorg. Chem.* **2001**, *40*, 5934–5941.
58. Reddy, P.A.N.; Nethaji, M.; Chakravarty, A.R. Ternary mononuclear and ferromagnetically coupled dinuclear copper(II) complexes of 1,10-phenanthroline and *N*-salicylidine-2-methoxyaniline that show supramolecular self-organization. *Eur. J. Inorg. Chem.* **2003**, 2318–2324.
59. Matoga, D.; Szklarzewicz, J.; Stadnicka, K.; Shongwe, M.S. Iron(III) complexes with a biologically relevant aroylhydrazone: crystallographic evidence for coordination versatility. *Inorg. Chem.* **2007**, *46*; 9042–9044.
60. Ali, M.S.; El-Saied, F.A.; Shakdofa, M.M.E.; Karnik, S.; Jaragh-Alhadad, L.A. Synthesis and characterization of thiosemicarbazone metal complexes: crystal structure, and proliferation activity against breast (MCF7) and lung (A549) cancers. *J. Mol. Struct.* **2023**, *1274*, 134485.
61. Latheef, L.; Manoj, E.; Kurup, M.R.P. Salicylaldehyde 4,4′-(hexane-1,6-diyl)-thiosemicarbazone. *Acta Cryst.* **2006**, *C62*, o16–o18.
62. Chattopadhyay, D.; Mazumdar, S.K.; Banerjee, T.; Ghosh, S.; Mak, T.C.W. Structure of salicylaldehyde thiosemicarbazone. *Acta Cryst.* **1988**, *C44*, 1025–1028.
63. Vrdoljak, V.; Cindrić, M.; Milić, D.; Matcović-Ćalogović, D.; Novak, P.; Kamenar, B. Synthwsis of five new molybdenum(VI) thiosemicarbazonato complexes. Crystal structures of salicylaldehyde and 3-methoxysalicylaldehyde 4-methylthiosemicarbazones and their molybdenum(VI) complexes. *Polyhedron* **2005**, *24*, 1717–1726.
64. Labisbal, E.; Haslow; K.D.; Sousa-Pedrares, Valdés-Martínez, J.; Hernández-Ortega, S.; West, D.X. Copper(II) and nickel(II) complexes of 5-methyl-2-hydroacetophenone *N*(4)-substituted thiosemicarbazones. *Polyhedron* **2003**, *22*, 2831–2837.
65. Kowol, C.R.; Reisner, E.; Chiorescu, I.; Arion, V.B.; galanski, M.; Deubel, D.V.; Keppler, B.K. An electrochemical study of antineoplatic gallium, iron, and ruthenium with redox noninnocent α-N-heterocyclic chalcogensemicarbazones. *Inorg. Chem.* **2008**, *47*, 11032–11047.
66. West, D.X.; Bain, G.A.; Butcher, R.J.; Jasinski, J.P.; Li, Y.; Pozdniakiv, R.Y.; Valdés-Martínez, J.; Toscano, R.A.; Hernández-Ortega, S. Structural studies of three isomeric forms of heterocyclic N(4)-substituted thiosemicarbazones and two nickel(II) complexes. *Polyhedron* **1996**, *15*; 665–674.
67. Kowol, C.R.; Eichinger, R.; Jakupec, M.A.; Galanski, M.S.;Arion, V.B.; Keppler, B.K. Effect of metal ion complexation and chalcogen donor identity on the antiproliferative activity of 2-acetylpyridine *N*,*N*-dimethyl(chalcogen)semicarbazones. *J. Inorg. Biochem.* **2007**, *101*, 1946–1957.
68. Usman, A.; Abdul Razak, I., Chantrapromma, S.; Fun, H.-K.; Philip, V.; Sreekanth, A.; Kurup, M.R.P. Di-2-pyridyl ketone N^4,N^4-(butane-1,4-diyl)thiosemicarbazone. *Acta Cryst.* **2002**, *C58*, 0652–o654.
69. Philip, V.; Suni, V.; Kurup, M.R.P. Di-2-pyridyl ketone 4-methyl-4-phenylthiosemicarbazone. *Acta Cryst.* **2004**, *C60*, o856-o858.
70. Geary, W.J. The use of conductivity measurements in organic solvents for the characterisation of coordination compounds. *Coord. Chem. Rev.* **1971**, *7*, 81–122.
71. Philip, V.; Manoj, E.; Kurup, M.R.P.; Nethaji, M. [Di-2-pyridyl ketone N^4,N^4-(butane-1,4-diyl)thiosemicarbazonato-κ^3N,$N'S$]dioxovanadium(V). *Acta Cryst.* **2005**, *C61*, m488–m490.
72. Gómez-Saiz, P.; García-Tojal, J.; Mendia, A.; Donnadieu, B.; Lezama, L.; Pizarro, J.L.; Arriortua, M.I.; Rojo, T. Coordination modes in a tridentate NNS (thiosemicarbazonato)copper(II) system containing oxygen-donor coligands – structures of [{Cu(L)(X)}$_2$] (X = formato, propionato, nitrito). *Eur. J. Inorg. Chem.* **2003**, 518–527.
73. Shongwe, M.S.; Al-Kharousi, H.N.R.; Adams, H.; Morris, M.J.; Bill, E. Unprecedented $[V_2O]^{6+}$ Core of a centrosymmetric thiosemicarbazonato dimer: spontaneous deoxygenation of oxovanadium(IV). *Inorg. Chem.* **2006**, *45*, 1103–1107.
74. Addison, A.W.; Rao, T.N.; Reedijk, J.; van Rijn, J., Verschoor, G.C. Synthesis, structure, and spectroscopic properties of copper(II) compounds containing nitrogen-sulphur donor ligands: the crystal and molecular structure of aqua[1,7-bis(N-methylbenzimidazol-2′-yl)-2,6-dithiaheptane]copper(II) perchlorate. *J. Chem. Soc., Dalton Trans.* **1984**, 1349–1356.

75. Bernhardt, P.V.; Sharpe, P.C.; Islam, M.; Lovejoy, D.B.; Kalinowski, D.S.; Richardson, D.R. Iron chelators, of the dipyridylketone thiosemicarbazone class: precomplexation, and transmetalation effects on anticancer activity. *J. Med. Chem.* **2009**, *52*, 407–415.
76. Anderson, O.P. Crystal and molecular structure of tris-(1,10-phenanthroline)copper(II) perchlorate. *J. Chem. Soc., Dalton*, **1973**, 1237–1241.
77. Burčák,M.; Potočňák, I.; Baran, P.; Jäger, L. Low-dimensional compounds containing cyano groups. X. (Dicyanamido-κN^1)bis(1,10-phenanthroline-$\kappa^2 N,N'$)copper(II) perchlorate. *Acta Cryst.* **2004**, *C60*, m601–m604.
78. Yang, L.; Powell, D.R.; Houser, R.P. Structural variation in copper(I) complexes with pyridylmethylamide ligands: structural analysis with a new four-coordinate geometry index, τ_4. *Dalton Trans.*, **2007**, 955–964.
79. Tei, L.; Blake, A.J.; Lippolis, V.; Wilson, C.; Schröder, M. Methanolysis of nitrile-functionalised pendant arm derivatives of 1,4,7-triazacyclononane upon coordination to Cu^{II}. *Dalton Trans.* **2003**, 304–310.
80. Su, S.-Y.; Liao, S.; Wanner, M.; Fiedler, J.; Zhang, C.; Kang, B.-S.; Kaim, W. The copper(I)/copper(II) transition in complexes with 8-alkylthioquinoline based multidentate ligands. *Dalton Trans.* **2003**, 189–202.
81. Tubbs, K. J.; Fuller, A.L.; Bennett, B.; Arif, A. M.; Makowska-Grzyska, M.M.; Berreau, L. M. Evaluation of the influence of a thioether substituent on the solid state and solution properties of N_3S-ligated copper(II) complexes. *Dalton Trans.* **2003**, 3111–3116.
82. Liu, Y.H.; Li, A.; Shao, J.; Xie, C.-Z.; Song, X.-Q.; Bao, W.-G.; Xu, J.-Y. Four Cu(II) complexes based on antitumour chelators: synthesis, structure, DNA binding/damage, HSA interaction and enhanced cytotoxicity. *Dalton Trans.* 2016, **45**, 8036–8049.
83. Ying, P.; Zeng, P. Lu, J.; Chen, H.; Liao, X.; Yang, N. New oxidovanadium complexes incorporating thiosemicarbazones and 1,10-phenanthroline dervatives as DNA cleavage, potential anticancer agents, and hydroxyl radical scavenger. *Chem. Biol. Drug. Des.* **2015**, *86*, 926–937.
84. Bruker, *SADABS*, Bruker Axs Inc., Madison, Wisconsin, USA 2016.
85. Krause, L.; Herbst-Irmer, R.; Sheldrick, G.M.; D. Stalke, D. *J. Appl. Crystallogr.*, **2015**, *48*, 3–10.
86. Sheldrick, G. M. SHELXT - Integrated Space-Group and Crystal-Structure Determination. *Acta Crystallogr. Sect. A Found. Crystallogr.* **2015**, 71, 3–8. https://doi.org/10.1107/S2053273314026370.
87. Sheldrick, G. M. Crystal Structure Refinement with SHELXL. *Acta Crystallogr. Sect. C Struct. Chem.* **2015**, 71 (Md), 3–8. https://doi.org/10.1107/S2053229614024218.
88. Dolomanov, O. V.; Bourhis, L. J.; Gildea, R. J.; Howard, J. A. K. K.; Puschmann, H. OLEX2: A Complete Structure Solution, Refinement and Analysis Program. *J. Appl. Crystallogr.* **2009**, 42 (2), 339–341. https://doi.org/10.1107/S0021889808042726.